Determination of rate constants for aqueous reactions of HCFC-123 and HCFC-225ca with OH^- along with Henry's law constants of several HCFCs

Shuzo Kutsuna [1]*

1. National Institute of Advanced Industrial Science and Technology (AIST),

16-1 Onogawa, Tsukuba, Ibaraki 305 8569, Japan

TITLE RUNNING HEAD: Hydrolysis rate constants of HCFC-123 and HCFC-225ca

ABSTRACT

Henry's law constants of six kinds of hydrochlorofluorocarbons (HCFCs) were determined at 313–353 K by means of a phase-ratio variation headspace method: $K_H = K_H^{353}\exp\left(-\frac{\Delta H_{sol}}{R}\left(\frac{1}{T}-\frac{1}{353}\right)\right)$ and (K_H^{353} in M atm^{-1}, ΔH_{sol} in kJ mol^{-1}) = (0.0070±0.0006, –23±2), (0.0038±0.0011, –22±10), (0.0065±0.0007, –21±3), (0.0026±0.0007, –23±8), (0.0016±0.0003, –30±4), and (0.0022±0.0003, –25±4), respectively, for HCFC-141b (CH_3CCl_2F), HCFC-142b (CH_3CClF_2), HCFC-123 (CF_3CHCl_2), HCFC-124 (CF_3CHClF), HCFC-225ca ($CF_3CF_2CHCl_2$), and HCFC-225cb ($CClF_2CF_2CHClF$). Errors represent 2 standard deviations only for the fitting. Decay of headspace partial pressures of these HCFCs via hydrolysis was discerned only for CF_3CHCl_2 and $CF_3CF_2CHCl_2$ under the experimental conditions examined. Rate constants (k_{OH}- in M^{-1} s^{-1}) for aqueous reactions of $CF_3CF_2CHCl_2$ and CF_3CHCl_2 with OH^- at 313–353 K were determined to be $(0.57\pm0.04)\exp\left(-(11300\pm600)\times\left(\frac{1}{T}-\frac{1}{353}\right)\right)$ and $(2.9\pm0.2)\times10^{-4}\exp\left(-(8800\pm900)\times\left(\frac{1}{T}-\frac{1}{353}\right)\right)$, respectively, from monitoring changes in headspace partial pressure over prescribed concentrations of aqueous NaOH as a function of headspace time duration and concentration of aqueous NaOH. The calculations performed included consideration of gas-water equilibrium and hydrolysis at both headspace and room temperatures. The calculation for CF_3CHCl_2 also included consideration of salting-out effects: the salting coefficient of NaCl on a natural-log basis was determined to be 0.36 ± 0.06 M^{-1} and this value was used for consideration of salting-out effect of NaOH. Whereas the activation energy for $CF_3CF_2CHCl_2$ was larger than that for CF_3CHCl_2, the k_{OH}- value at 353 K of $CF_3CF_2CHCl_2$ was 10^3 times larger than that of CF_3CHCl_2, indicating that reaction mechanisms for these two HCFCs differed from each other. The aqueous reaction of $CF_3CF_2CHCl_2$ with OH^- was found to proceed through dehydrofluorination on the basis of detection of $CF_3CF{=}CCl_2$ as a primary degradation product of the reaction and proportionality of the rate constants to both concentrations of $CF_3CF_2CHCl_2$ and OH^-.

KEYWORDS.

Hydrochlorofluorocarbon, CF_3CHCl_2, $CF_3CF_2CHCl_2$, Solubility, Hydrolysis, Dehydrofluorination.

Introduction

Hydrochlorofluorocarbons (HCFCs) have been used to replace chlorofluorocarbons (CFCs) for several applications because the former have shorter lifetimes in the atmosphere and consequently have lower stratospheric ozone depletion potentials (ODPs) than the latter (*1*). Nevertheless, under the Montreal Protocol and its subsequent amendments (*2*), HCFC consumption is due to be phased out by 2020 for developed countries and by 2030 for developing countries owing to HCFCs' classification as ODSs (Ozone-Depleting Substances). In compliance with the Montreal Protocol, discarded HCFC-containing equipment is collected and the HCFCs are extracted and destroyed at specified ODS destruction facilities, including rotary kilns such as in-service rotary kiln waste incinerators.

In a previous study (*3*), the author and coworkers found that the rate constants for HCFC-22 ($CHClF_2$) hydrolysis with OH^- (k_{OH^-}) at 353 K were 10 times larger than had been reported before, and thus concluded that alkaline wet scrubbers could be used to remove residual $CHClF_2$ in the wet flue gas cleaning system of ODS destruction facilities. We further noted that hydrolysis is a potential technique for destruction of $CHClF_2$. In this study, the author examined the hydrolysis of the following six commercial HCFCs: HCFC-141b (CH_3CCl_2F), HCFC-142b (CH_3CClF_2), HCFC-123 (CF_3CHCl_2), HCFC-124 (CF_3CHClF), HCFC-225ca ($CF_3CF_2CHCl_2$), and HCFC-225cb ($CClF_2CF_2CHClF$). Because the determination of k_{OH^-} requires input of Henry's law constant (K_H), the K_H values of the HCFCs were determined at 313−353 K by means of the phase-ratio variation headspace (PRV-HS) method (*4*) in a similar way as determined previously for $CHClF_2$ (*3*). The k_{OH^-} values of CF_3CHCl_2 and $CF_3CF_2CHCl_2$ were determined at 313−353 K, whereas hydrolysis of the other HCFCs was not detectable under the experimental conditions examined. In terms of the Henry's law constants and the rate constants determined, the author notes hydrolysis as a potential control technique for some HCFCs.

Experimental Methods

Materials

HCFC standard gas mixtures (diluted with synthetic air) were purchased from Takachiho Kogyou Co. Ltd. (Tokyo, Japan). The concentration of each standard gas mixture was 1000 ppmv (CH_3CCl_2F), 1020 ppmv (CH_3CClF_2), 959 ppmv (CF_3CHCl_2) and 1140 ppmv (CF_3CHClF). For $CF_3CF_2CHCl_2$ and $CClF_2CF_2CHClF$, a synthetic mixture of $CF_3CF_2CHCl_2$, $CClF_2CF_2CHClF$, and air was used, the concentrations of $CF_3CF_2CHCl_2$ and $CClF_2CF_2CHClF$ being 1070 ppmv and 1310 ppmv, respectively. Test sample concentrations were set at about 2–13 ppmv by dilution of the HCFC standard gas mixture with ambient air.

Standard aqueous solutions of 5 M and 1 M sodium hydroxide (NaOH) were purchased from Wako Pure Chemical Industries (Osaka, Japan). Water was purified with a Millipore Milli-Q Gradient A10

system (>18 MΩ).

Determination of Henry's law constants

Henry's law constants of HCFCs were determined by the PRV-HS method in a way similar to that used in the previous study (*3*). The determination was carried out with an automatic headspace sampler (HP7694, Agilent Technologies, Palo Alto, CA) connected to a gas chromatograph mass spectrometer (GC-MS; Agilent GC6890N with 5973inert, Agilent Technologies, Palo Alto, CA). Headspace temperatures ranged from 313 to 353 K in intervals of 10 K. The headspace samples were continuously shaken slowly by a mechanical set-up for headspace equilibration time, and then headspace gas (1 cm^3) was injected into the GC in split mode (split ratio = 1:30 or 1:20).

The time necessary to attain equilibration between the headspace and the aqueous solution was determined by analyzing the headspaces over test samples as a function of time until steady-state conditions were attained (*5*). Figure S1 plots the relative signal intensity of GC-MS peak areas for each HCFC, that is, the ratio of the headspace partial pressure at time t to that at 60 min (P_t /P_{60}), against the time (t_h) during which samples were placed in the headspace oven. The graph shows no increase or decrease in the peak area after about 30 minutes. Therefore, we set the headspace equilibration time at 1 h for all the measurements.

GC-MS peaks due to HCFCs were measured in selected-ion mode. A PoraBOND-Q capillary column (0.32-mm i.d. × 50 m length, Agilent Technologies Inc., Palo Alto, CA) was used to separate the HCFCs; an Rts-1 capillary column (0.32-mm i.d. × 60 m length, 1.5-μm film thickness, Restek, Co., Bellefonte, PA) was also used to separate $CF_3CF_2CHCl_2$ and $CClF_2CF_2CHClF$. The selected ions and the column temperatures used in each experiment are listed in Table S1. Helium was used as the carrier gas. The injection port was kept at 383 K.

Headspace samples, which contained five different amounts of each HCFC and six different volumes of water, were prepared for each temperature as follows (30 samples total). Volumes (V_i) of 1.5, 3.0, 4.5, 6.0, 7.5, and 9.0 cm^3 of Milli-Q water were pipetted into six headspace vials with a total volume (V) of 21.4 cm^3 (V_i/V = 0.070, 0.140, 0.210, 0.280, 0.350, and 0.421, respectively). Five sets of the six headspace vials were prepared and sealed. A prescribed volume (v_j) of a standard gas mixture of HCFC and air was added to a set of five vials containing the same volume (V_i) of water by means of a gastight syringe (v_j = 0.05, 0.10, 0.15, 0.20, or 0.25 cm^3).

If P_{ij} is the equilibrium partial pressure in atm for a HCFC sample in a vial with volume V in cm^3 containing V_i cm^3 of water and v_j cm^3 of HCFC gas mixture added, and if P_j is the equilibrium partial pressure in atm for the HCFC in a sample containing v_j cm^3 of HCFC gas mixture without water, then Eq. 1 applies:

$$\frac{P_j V}{RT} = K_{\mathrm{H}}(T) P_{ij} V_i + \frac{P_{ij}(V - V_i)}{RT} \quad (1)$$

where $K_{\mathrm{H}}(T)$ is the Henry's law constant in M atm^{-1} at temperature T in K and R is the gas constant (0.0821 dm^3 atm K^{-1} mol^{-1}).

Because the signal peak area of the HCFC (S_{ij}) at partial pressure P_{ij} is expected to be proportional to v_j for each set of samples with the same V_i, a plot of S_{ij} *versus* v_j should be a straight line intercepting the origin according to Eq. 2.

$$S_{ij} = L_i v_j \quad (2)$$

The slope of each line, denoted as L_i, corresponds to P_{ij} at V_i = 1.0 cm^3. Letting L be the slope corresponding to P_i at V_i = 1.0 cm^3, Eq. 3 applies.

$$\frac{1}{L_i} = \frac{1}{L} + \frac{RT K_{\mathrm{H}}(T) - 1}{L} \frac{V_i}{V} \quad . \quad (3)$$

Plotting $\frac{1}{L_i}$ against $\frac{V_i}{V}$ gives an intercept of $\frac{1}{L}$ and a slope of $\frac{RT K_{\mathrm{H}}(T) - 1}{L}$, and $K_{\mathrm{H}}(T)$ is obtained from these two values. Therefore, $K_{\mathrm{H}}(T)$ can be determined by recording the peak area S_{ij} and deriving L_i from a plot of S_{ij} *vs.* v_j and then applying regression analysis to the plots of $\frac{1}{L_i}$ versus $\frac{V_i}{V}$ with respect to Eq. 3. In other words, the absolute headspace concentration of HCFC does not need to be known.

Because, as described later, high concentrations of aqueous NaOH (i.e., 0.5–3 M) were used to determine the k_{OH^-} of CF_3CHCl_2, the salting-out coefficient was estimated for the k_{OH^-} of CF_3CHCl_2 by using aqueous NaCl solutions.

Determination of rate constants for aqueous reactions with OH$^-$

To evaluate the hydrolysis of the HCFCs, changes in headspace partial pressures were examined as a function of headspace time duration over a 1M NaOH aqueous solution at 353 K. As described in the *Results and Discussion* section, only two HCFCs, $CF_3CF_2CHCl_2$ and CF_3CHCl_2, exhibited a decrease in headspace partial pressure. For these two HCFCs, k_{OH^-} values were determined at 313–353 K in intervals of 10 K in a way similar to that applied in the previous study (*3*). The determination of k_{OH^-} values was carried out by means of an automatic headspace sampler connected to a gas chromatograph/mass spectrometer. A gas chromatograph with a flame ionization detector (FID-GC;

Agilent GC6890N with 5973inert, Agilent Technologies, Palo Alto, CA) was also used with a Rts-1 wide-bore column (0.53-mm i.d. × 30 m length, Restek, Co., Bellefonte, PA) for estimating the conversion ratio of $CF_3CF_2CHCl_2$ into its degradation product.

A series of headspace samples (typically, 8 samples) containing a prescribed volume (typically, 9.0 cm^3) and a prescribed concentration of aqueous NaOH solution were prepared for each temperature. The concentration of NaOH was set at 1−4 mM for $CF_3CF_2CHCl_2$ and at 0.5−3 M for CF_3CHCl_2 by dilution of a 1 or 5 M standard aqueous NaOH solution with water. The same amount of the HCFC standard gas was added to each sealed test sample; the concentration of $CF_3CF_2CHCl_2$ or CF_3CHCl_2 corresponded to ca. 13 ppmv if aqueous NaOH was absent. The time during which samples were placed in the headspace oven (t_h) was set at 1–12 h ($CF_3CF_2CHCl_2$) or 1–8 h (CF_3CHCl_2) and differed among samples, and then the signal peak area of $CF_3CF_2CHCl_2$ or CF_3CHCl_2 (S_t) was measured for a series of samples as a function of t_h. During this time duration, the headspace samples were continuously shaken slowly by a mechanical set-up. Because the temperature of the headspace samples reached the set temperature within 40 min, S_t decayed exponentially with respect to t_h when t_h was longer than 40 min, as shown in Eq. 4:

$$\frac{d\,S_t}{d\,t} = -k_1^{(g)}(T)S_t \tag{4}$$

where $k_1^{(g)}(T)$ is the first-order rate constant for decay of $CF_3CF_2CHCl_2$ or CF_3CHCl_2 in the gas phase (headspace) at temperature T in K. Integrating Eq. 4 with respect to t from 1 h to t_h gives Eq. 4′:

$$\ln(S_t) = \mathrm{A}_1 - k_1^{(g)}(T)t_h \tag{4′}$$

where A_1 is a constant that is common to each series of headspace samples. When the gas-water equilibrium of $CF_3CF_2CHCl_2$ or CF_3CHCl_2 is established, the rate constant of decay is given by Eq. 5:

$$k_1^{(g)}(T) = \frac{k_1^{(l)}(T)}{Q_i(T)} \tag{5}$$

where $Q_i(T)$ is given by Eq. 6, and $k_1^{(l)}(T)$ is a pseudo-first-order rate constant for hydrolysis of $CF_3CF_2CHCl_2$ or CF_3CHCl_2 in water at temperature T and is expressed by Eq. 7.

$$Q_i(T) = 1 + \frac{1}{K_H^*(T)RT}\left(\frac{V}{V_i} - 1\right) \tag{6}$$

$$k_1^{(l)}(T) = k_{OH^-}(T)[OH^-] + k_N(T) \tag{7}$$

where $K_H^*(T)$ is a Henry's law constant that accounts for the salting-out effect; and $k_{OH^-}(T)$ and $k_N(T)$ are rate constants for aqueous reactions of $CF_3CF_2CHCl_2$ or CF_3CHCl_2 with OH^- and water, respectively, at temperature T. Because $k_N(T)$ is negligible compared to the quantity ($k_{OH^-}(T)$ [OH^-]) under the experimental conditions used in this study, Eqs. 5 and 7 can be combined to give Eq. 5′.

$$k_1^{(g)}(T) = \frac{k_1^{(l)}(T)}{Q_i(T)} = \frac{k_{OH^-}(T)[OH^-]}{Q_i(T)} \tag{5′}$$

Notably, Eq. 4′ must be corrected to account for hydrolysis that might have occurred at room temperature before the sample vial was placed in the headspace oven. The duration (t_r) during which the sample was kept at room temperature (298 ± 2 K) before being placed in the headspace oven differed between experimental runs. Hydrolysis of $CF_3CF_2CHCl_2$ or CF_3CHCl_2 at room temperature might have been significant, especially for experimental runs with lower headspace temperatures such as 313 K. Hence, Eq. 4′ was replaced by Eq. 8:

$$\ln(S_t) = A_2 - k_1^{(g)}(T)t_h - k_1^{(g)}(298)t_r = A_2 - k_1^{(g)}(T)t_m \tag{8}$$

where A_2 is a constant, which is common to each series of headspace samples, and t_m is given by Eq. 9:

$$t_m = t_h + \frac{k_1^{(g)}(298)}{k_1^{(g)}(T)} t_r . \tag{9}$$

Combining Eqs. 5′ and 9 gives Eq. 10:

$$t_m = t_h + \frac{k_{OH^-}(298)}{k_{OH^-}(T)} \frac{Q_i(T)}{Q_i(298)} t_r = t_h + \exp\left[-\frac{\Delta E_a}{R}\left(\frac{1}{298} - \frac{1}{T}\right)\right] \frac{Q_i(T)}{Q_i(298)} t_r \tag{10}$$

where ΔE_a is the activation energy for aqueous reaction of $CF_3CF_2CHCl_2$ or CF_3CHCl_2 with OH^-, as expressed by Eq. 11 (Arrhenius equation):

$$k_{OH^-}(T) = A \exp\left(-\frac{\Delta E_a}{RT}\right) \tag{11}$$

where A is the Arrhenius parameter. Eq. 11 can be represented using the k_{OH^-} value at 353 K by Eq. 11′.

$$k_{OH^-}(T) = k_{OH^-}(353) \exp\left[-\frac{\Delta E_a}{R}\left(\frac{1}{T} - \frac{1}{353}\right)\right] \tag{11′}$$

Values of $k_1^{(g)}$ were determined from nonlinear regression of plots of S_t versus t_h with Eq. 4′, and then values of $k_1^{(l)}$ were calculated from the $k_1^{(g)}$ values and $Q_i(T)$ with Eq. 5. Linear regression of the obtained $k_1^{(l)}(T)$ values versus NaOH concentration with weighting (error)$^{-2}$ at each temperature yielded a series of k_{OH}-(T) values at different temperatures. Nonlinear regression of the temperature dependence of the k_{OH}-(T) values with weighting (error)$^{-2}$ according to Eq. 11 gave ΔE_a. ΔE_a was used to calculate t_m with Eq. 10, and nonlinear regression of plots of S_t versus t_m with Eq. 8 gave $k_1^{(g)}$. This procedure was repeated until both $k_{OH^-}(T)$ and ΔE_a converged.

In the previous study, the author et al. (*3*) made an additional correction of Eq. 5′ to account for aqueous-phase diffusion. However, in this work the author made no additional correction because the data were fit well by Eq. 5′ as shown below in the *Results and Discussion* section.

Results and Discussion

Determination of Henry's law constants

Fig. S2A plots the peak area (S_{ij}) against the volume of CH_3CCl_2F gas mixture added (v_j) for samples of CH_3CCl_2F with V_i = 9.0, 7.5, 6.0, 4.5, 3.0, and 1.5 cm^3 at 343 K. The data obtained for each V_i form a straight line intersecting the origin, indicating that S_{ij} was proportional to v_j for vials with the same value of V_i. The slope (L_i) of each line was obtained by linear regression with respect to Eq. 2, and the reciprocal slope (L_i^{-1}) was plotted against the phase ratio (V_i/V) as shown in Fig. S2B. Errors of L_i indicate two standard deviations only for the regression.

Plots of L_i^{-1} and V_i/V obey Eq. 3. The slopes, intercepts, and correlation coefficients for linear regression with weighting (error)$^{-2}$ with respect to Eq. 3 are given along with the $K_H(T)$ values calculated from the slopes and intercepts in Table S2: Table S2 also lists the corresponding values for CH_3CCl_2F at the other temperatures. The corresponding values of CH_3CClF_2, CF_3CHCl_2, CF_3CHClF, $CF_3CF_2CHCl_2$, and $CClF_2CF_2CHClF$ are listed in Tables S3, S4, S5, S6, and S7, respectively. For $CF_3CF_2CHCl_2$ and $CClF_2CF_2CHClF$, errors of K_H were relatively large because the values of K_H were small ($<5 \times 10^{-3}$ M atm^{-1}). Quadruple measurements of K_H were hence carried out at each temperature and the K_H value at each temperature was determined to be the average of the quadruple measurements with weighting (error)$^{-2}$.

Fig. 1 shows the temperature dependence of $K_H(T)$ values determined in this study for CH_3CCl_2F, CH_3CClF_2, CF_3CHCl_2, and CF_3CHClF, along with values reported in the literature (*6*, *7*). Fig. 2 shows the temperature dependence of $K_H(T)$ values determined in this study for $CF_3CF_2CHCl_2$ and $CClF_2CF_2CHClF$. The temperature-dependence of $K_H(T)$ is generally represented by the van't Hoff equation (Eq. 12):

$$K_{\mathrm{H}}(T) = K_{\mathrm{H}}(T_0)\exp\left[-\frac{\Delta H_{\mathrm{sol}}}{R}\left(\frac{1}{T}-\frac{1}{T_0}\right)\right] \quad (12)$$

where T_0 is a prescribed temperature, for example, 353 K; $K_{\mathrm{H}}(T_0)$ is the Henry's law constant at temperature T_0; and ΔH_{sol} is the enthalpy of dissolution of HCFC into water. As shown in Figs. 1 and 2, the relationship between $\ln(K_{\mathrm{H}}(T))$ and T^{-1} for each HCFC was linear in the temperature range examined and obeyed Eq. 12. The plot of $K_{\mathrm{H}}(T)$ versus T^{-1} was nonlinearly fitted with weighting $(\text{error})^{-2}$ with respect to Eq. 12 to determine $K_{\mathrm{H}}(353)$, $K_{\mathrm{H}}(298)$ and ΔH_{sol}. Table I lists the $K_{\mathrm{H}}(353)$, $K_{\mathrm{H}}(298)$ and ΔH_{sol} values determined. The error represents two standard deviations only for the fitting. Table I also lists the corresponding values reported in the literature (*6*, *7*).

As shown in Fig. 1 and Table I, the $K_{\mathrm{H}}(T)$ values obtained for CH_3CClF_2 and CF_3CHClF are, within experimental error, in good agreement with the reported values. In contrast, although the $K_{\mathrm{H}}(T)$ values obtained for CF_3CHCl_2 are in agreement with the reported values at the higher temperatures examined, such as 353 K, the $K_{\mathrm{H}}(T)$ values for CF_3CHCl_2 were smaller than the reported values by several tens of percent at lower temperatures examined, such as 313 K,. The reason for this difference is unclear. In addition, the $K_{\mathrm{H}}(T)$ values obtained for CH_3CCl_2F were an order of magnitude larger than the reported values. The resulting values of ΔH_{sol} for CH_3CCl_2F were significantly different as well, with the previously published value somewhat out of line with others. Although the solubility of CH_3CCl_2F in water is expected to be larger than that of CH_3CClF_2 because CH_3CCl_2F has one more Cl atom and one less F atom than CH_3CClF_2, the reported $K_{\mathrm{H}}(T)$ values for CH_3CCl_2F are smaller than those of CH_3CClF_2; hence, the reported $K_{\mathrm{H}}(T)$ values for CH_3CCl_2F might have been underestimated. To the author's knowledge, the data shown in Fig. 2 and Table I are the first reported $K_{\mathrm{H}}(T)$ values for $CF_3CF_2CHCl_2$ and $CClF_2CF_2CHClF$.

Headspace partial pressures of CH_3CCl_2F, CH_3CClF_2, CF_3CHClF, and $CClF_2CF_2CHClF$ over 1M aqueous NaOH at 353 K

Fig. S3 shows changes in relative headspace partial pressures of CH_3CCl_2F, CH_3CClF_2, CF_3CHClF, and $CClF_2CF_2CHClF$ as a function of headspace equilibration time (t_{h}) at 353 K for V_i = 9.0 cm^3 of 1 M aqueous NaOH. The ordinate (P_t/P_{60}) indicates the ratio of the headspace partial pressure at time $t = t_{\mathrm{h}}$ to that at 60 min. The P_t values remained almost constant: application of Eq. 4′ to the data gave $k_1^{(\mathrm{g})} = -(2.1\pm3.8) \times 10^{-6}$, $-(1.3\pm7.4) \times 10^{-6}$, $(1.9\pm3.6) \times 10^{-6}$, and $-(2.7\pm4.0) \times 10^{-6}$ s^{-1}, respectively, for CH_3CCl_2F, CH_3CClF_2, CF_3CHClF, and $CClF_2CF_2CHClF$ (errors represent two standard deviations only for the fitting). In other words, decay of these HCFCs was not observed within the reported errors. Upper limit value of k_{OH^-}, which is designated as $\mathrm{U}(k_{\mathrm{OH}^-})$ hereafter, was evaluated from Eq. 5′. Since the $Q_i(\mathrm{T})$ values were calculated to be 7.8±0.6, 13.5±3.6, 19.3±4.9, and 22.6±3.0, respectively, for

CH_3CCl_2F, CH_3CClF_2, CF_3CHClF, and $CClF_2CF_2CHClF$ by use of Eq. 6 and the $K_H(T)$ values listed in Table I, U(k_{OH^-}) values in M^{-1} s^{-1} were calculated to be 4.6×10^{-5}, 1.2×10^{-4}, 3.3×10^{-5}, and 1.5×10^{-4}, respectively, for CH_3CCl_2F, CH_3CClF_2, CF_3CHClF, and $CClF_2CF_2CHClF$.

In contrast, as shown in Figs. 3 and 4, $CF_3CF_2CHCl_2$ and CF_3CHCl_2 decreased through aqueous reaction with OH^-. In particular, decay of $CF_3CF_2CHCl_2$ could be discerned for samples containing much lower concentrations (1–4 mM) of aqueous NaOH. Rate constants for aqueous reactions of $CF_3CF_2CHCl_2$ and CF_3CHCl_2 with OH^- were determined at 313–353 K as described in the following sections.

Determination of rate constants for aqueous reactions of $CF_3CF_2CHCl_2$ with OH^- via Eqs. 4′ and 8

Changes in P_t/P_{60} for $CF_3CF_2CHCl_2$ were examined as a function of t_h at 313–353 K for V_i = 9.0 cm^3 of 1, 2, 3, and 4 mM aqueous NaOH. Fig. 3A plots the data at 353 K. The $k_1^{(g)}$ values were determined by regression of the P_t/P_{60} values versus t_h with Eq. 4′ for each NaOH concentration. The $k_1^{(l)}$ values were calculated from $k_1^{(g)}$ values by means of Eq. 5′ by using the calculated Q_i value and were plotted against NaOH concentration (Fig. 3B). The Q_i values were calculated with Eq. 5 from $K_H(T)$ deduced from Eq. 12. The errors ($\delta k_1^{(l)}$) represent both two standard deviations for the linear regression ($\delta_r k_1^{(g)}$) and the errors due to two standard deviations of $Q_i(T)$ ($\delta Q_i(T)$); that is, $\delta k_1^{(l)} = k_1^{(l)} \sqrt{\left(\frac{\delta_r k_1^{(g)}}{k_1^{(g)}}\right)^2 + \left(\frac{\delta Q_i(T)}{Q_i(T)}\right)^2}$. As shown in Fig. 3B, the $k_1^{(l)}$ values were nearly proportional to the NaOH concentrations. Linear regression of the data with weighting $(error)^{-2}$ with respect to Eq. 5′ gave the k_{OH^-} values. Fig. S4 plots P_t/P_{60} against t_h (panels A1–A4) and plots $k_1^{(l)}$ against NaOH concentration (panels B1–B4) at 313–343 K. Table II lists the k_{OH^-} values obtained at 313–353 K. Figure 5 shows an Arrhenius plot of the k_{OH^-} values thus obtained. The ΔE_a values were obtained by nonlinear regression weighting $(error)^{-2}$ with respect to Eq. 11, and are listed in Table II. Furthermore, the k_{OH^-} values were corrected for hydrolysis at room temperature as follows.

The influence of hydrolysis of $CF_3CF_2CHCl_2$ at room temperature (298 ± 2 K) prior to the sample being placed in the headspace oven was taken into account to obtain $k_1^{(l)}$ (Fig. 3B; iteration processes were carried out with Eq. 8 as described in the *Experimental Methods* section). The $Q_i(298)$ value was calculated to be 5.5 ± 0.7 from Eq. 5 by using $K_H(298)$, which was calculated from Eq. 12 (Table I). Closed symbols in panels A in Figs. 3 and S4 plot P_t against $t = t_m$. Values of t_m were calculated from the convergence value of ΔE_a with Eq. 10. The $k_1^{(g)}$ values were obtained by nonlinear regression of the data of P_t/P_{60} versus t_m with Eq. 8 for each NaOH concentration. The $k_1^{(l)}$ values, which were calculated from the $k_1^{(g)}$ values and Q_i, were plotted against aqueous NaOH concentrations in panels B of Figs. 3 and S4. The $k_1^{(l)}$ values were proportional to NaOH concentrations at each temperature within the NaOH

concentration range examined. Linear regression of the data with weighting (error)$^{-2}$ with respect to Eq. 5′ gave the k_{OH^-} values.

Table II lists the corrected k_{OH^-} values obtained at 313–353 K along with the ΔE_a value obtained by convergence in the iteration process. Fig. 5 shows an Arrhenius plot of the k_{OH^-} values obtained. The $k_{OH^-}(T)$ values of $CF_3CF_2CHCl_2$ were eventually determined to be $(0.575 \pm 0.043)\exp\left(-(11300 \pm 620)\times\left(\frac{1}{T}-\frac{1}{353}\right)\right)$ in M^{-1} s^{-1}. The $k_{OH^-}(T)$ value at 353 K (0.58 ± 0.04 M^{-1} s^{-1}) and the ΔE_a value (94 ± 5 kJ mol^{-1}) for $CF_3CF_2CHCl_2$ determined here were as large as those determined for $CHClF_2$ (0.64 ± 0.10 M^{-1} s^{-1} and 93 ± 14 kJ mol^{-1}) in the previous study (*3*).

A degradation product for aqueous reactions of $CF_3CF_2CHCl_2$ with OH^-

A GC peak due to a reaction product was detected at a retention time earlier than that of $CF_3CF_2CHCl_2$. This reaction product is denoted *product X* hereafter. FID-GC measurements were run on headspace test samples of $CF_3CF_2CHCl_2$, which contained 9.0 cm^3 of 1 or 2 mM aqueous NaOH, for evaluating conversion ratios of $CF_3CF_2CHCl_2$ into *product X*. The quantities $S_{HCFC\text{-}225ca}(t_h)$ and $S_X(t_h)$ represent the FID signal intensity of $CF_3CF_2CHCl_2$ and of *product X*, respectively, at time t_h. Fig. 6A plots $S_X(t_h)$ against $\Delta S_{HCFC\text{-}225ca}(t_h)$, where $\Delta S_{HCFC\text{-}225ca}(t_h) = S_{HCFC\text{-}225ca}(0) - S_{HCFC\text{-}225ca}(t_h)$. The data display a linear relationship with a slope of 0.91 ± 0.06 between $S_X(t_h)$ and $\Delta S_{HCFC\text{-}225ca}(t_h)$. This linear relationship indicates that *product X* is a primary product consisting of three carbon atoms from $CF_3CF_2CHCl_2$, because FID signal intensity is generally proportional to the carbon number of organic samples.

Fig. 6B shows a mass spectrum of *product X*. Because the peak at m/z = 182 corresponds to $C_2F_4CCl_2^+$, *product X* can be identified as $CF_3CF{=}CCl_2$. Other peaks are reasonably assigned to fragment ions of $CF_3CF{=}CCl_2$: m/z = 69 (CF_3^+), 78 ($CFCCl^+$), 93 ($CF_3C_2^+$), 147 ($C_2F_4CCl^+$), and 163 ($C_2F_3CCl_2^+$). The peak at m/z = 132 is probably due to $CF_2CCl_2^+$ following rearrangement of fluorine and elimination of CF_2 as $CF^2CH_2^+$ is formed from $CF_3CF{=}CH_2^+$ (*8*). Accordingly, aqueous reaction of $CF_3CF_2CHCl_2$ with OH^- is found to proceed through dehydrofluorination (*9*). Because aqueous reactions of $CF_3CF_2CHCl_2$ with OH^- followed second-order kinetics, first-order in $CF_3CF_2CHCl_2$ and first-order in OH^-, as shown in Fig. 3, aqueous reaction of $CF_3CF_2CHCl_2$ with OH^- probably proceeds through base-promoted dehydrofluorination (*9, 10*) such as $CF_3CF_2CHCl_2 + OH^- \rightarrow CF_3CF{=}CCl_2 + F^- + H_2O$.

Determination of rate constants for aqueous reactions of CF_3CHCl_2 with OH^- via Eqs. 4′ and 8

The k_{OH^-} values of CF_3CHCl_2 were determined at 313–353 K in a similar way as aforementioned for $CF_3CF_2CHCl_2$ except that gas-water equilibrium included consideration of the salting-out effect.

Because CF_3CHCl_2 hydrolysis occurred at a substantially slower rate than that of $CF_3CF_2CHCl_2$, higher concentrations of aqueous NaOH, such as 1 M, were used to determine the hydrolysis rates of CF_3CHCl_2; therefore, the salting-out effect could have been significant and needed to be included in calculations for accurate determination of k_{OH^-} values. The salting-out effect was represented by the Setchinow-Harned-Owen equation, as follows (*11*):

$$\ln\left(\frac{K_H{}^0}{K_H{}^{m_s}}\right) = k_s m_s \tag{13}$$

where $K_H{}^0$ and $K_H{}^{m_s}$ are the Henry's law constant and the apparent Henry's law constant, respectively, for water having an ionic molality m_s (in mol kg^{-1}) of salt *S*, and k_s is a salting coefficient of salt *S* expressed on a natural-log basis. The salting-out effect was estimated by use of aqueous NaCl solutions instead of aqueous NaOH solutions. An ionic molality m_s was approximated by ionic molarity m_s (in M) here. The apparent K_H values were determined at 313, 333, and 353 K for test samples containing 9.0 cm^3 of 1 and 2 M aqueous NaCl solutions. The determination was performed twice for each NaCl concentration at each temperature. Fig. S6 plots the average of each set of two data points against NaCl concentration. Because the temperature dependence of k_s was unclear, linear regression was applied to all the data with weighting $(\text{error})^{-2}$ with respect to Eq. 13 to give $k_s = 0.36 \pm 0.06$ M^{-1}. The errors represent two standard deviations only for the regression. The apparent Henry's law constants, $K_H(T)^*$, were calculated with Eq. 13 from the evaluated k_s value, $K_H(T)$, and concentration of NaOH; $K_H(T)^*$ values were used to deduce $k_1^{(l)}$ from $k_1^{(g)}$ with Eq. 5.

Changes in P_t/P_{60} for CF_3CHCl_2 were examined as a function of t_h and t_m at 313–353 K for $V_i = 9.0$ cm^3 in a similar way as aforementioned for $CF_3CF_2CHCl_2$. Fig 4A plots P_t/P_{60} against t_h and t_m at 353 K. Fig. 4B plots the $k_1^{(l)}$ values determined from the data of P_t/P_{60} versus t_h or t_m against NaOH concentration. Fig. S5 plots P_t/P_{60} against t_h and t_m (panels A1–A4) and $k_1^{(l)}$ against NaOH concentration (panels B1–B4) at 313–343 K. The $k_1^{(l)}$ values were mostly proportional to NaOH concentration at each temperature within the NaOH concentration range examined. Linear regression of the data with weighting $(\text{error})^{-2}$ with respect to Eq. 5′ gave the k_{OH^-} values.

Table II lists the k_{OH^-} values of CF_3CHCl_2 thus corrected at 313–353 K along with the ΔE_a value obtained by convergence in the iteration process. Fig. 5 shows an Arrhenius plot of the k_{OH^-} values of CF_3CHCl_2 thus obtained. The $k_{OH^-}(T)$ values of CF_3CHCl_2 were eventually determined to be $(2.90 \pm 0.15) \times 10^{-4} \exp\left(-(8770 \pm 910) \times \left(\frac{1}{T} - \frac{1}{353}\right)\right)$ in M^{-1} s^{-1}: The k_{OH^-} value at 353 K was (2.90 ± 0.15) × 10^{-4} M^{-1} s^{-1} and the ΔE_a value was 73 ± 8 kJ mol^{-1}.

Comparison of $CF_3CF_2CHCl_2$ and CF_3CHCl_2 aqueous reactions with OH^-

The k_{OH^-} value at 353 K of $CF_3CF_2CHCl_2$ was 10^3 larger than that of CF_3CHCl_2, although the ΔE_a value of $CF_3CF_2CHCl_2$ was larger than that of CF_3CHCl_2. With the intention of understanding the difference between aqueous reactions of $CF_3CF_2CHCl_2$ and CF_3CHCl_2, with OH^-, the free energy, enthalpy, and the entropy of activation for the aqueous reactions were evaluated from the k_{OH^-} values and the ΔE_a values obtained. According to transition state theory, k_{OH^-} is given by Eq. 14:

$$k_{OH^-} = \frac{k_B T}{h} \exp\left(-\frac{\Delta G^{\ddagger}}{R T}\right) \tag{14}$$

where $\Delta G^{\ddagger}$ is the free energy of activation, k_B is Boltzmann's constant, and h is Planck's constant. Letting the enthalpy and the entropy of activation be $\Delta H^{\ddagger}$ and $\Delta S^{\ddagger}$, respectively, Eqs. 15 and 16 apply:

$$\Delta H^{\ddagger} = \Delta E_a + RT \tag{15}$$

$$\Delta G^{\ddagger} = \Delta H^{\ddagger} - T\Delta S^{\ddagger} \tag{16}$$

Values of $\Delta G^{\ddagger}$, $\Delta H^{\ddagger}$, and $\Delta S^{\ddagger}$ can be calculated from k_{OH^-} and ΔE_a with use of Eqs. 14–16 at each temperature and are listed for $CF_3CF_2CHCl_2$ and CF_3CHCl_2 in Table S8. There is a definitive difference in entropy of activation: ca. 7 J K^{-1} mol^{-1} for $CF_3CF_2CHCl_2$ and ca. –115 J K^{-1} mol^{-1} for CF_3CHCl_2. This difference indicates that reaction mechanisms for aqueous reactions of $CF_3CF_2CHCl_2$ and CF_3CHCl_2 with OH^- should be different.

As mentioned earlier, aqueous reactions of $CF_3CF_2CHCl_2$ with OH^- proceed through dehydrofluorination, and they displayed second-order kinetics, first-order in $CF_3CF_2CHCl_2$ and first-order in OH^-. The reaction mechanism that satisfies these characteristics includes E2 and two E1cB mechanisms [*10*]. In the E2 mechanism, both the C–H and C–F bonds cleave simultaneously via a single transition state. In the E1cB mechanisms, the C–H bond is ruptured prior to scission of the C–F bond (Eq. 17):

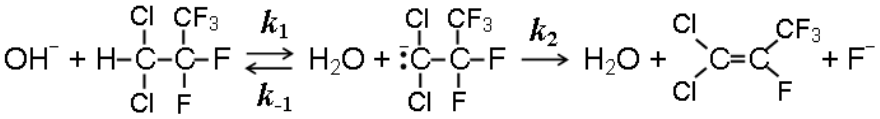

(17)

Depending upon the relative magnitudes of k_1, k_{-1}, and k_2, three distinct possibilities for base-promoted olefin formation by E1cB mechanisms exist: reversible E1cB or $(E1cB)_R$; irreversible E1cB or $(E1cB)_I$;

and E1. The E1 mechanism is not considered here because it does not display second-order kinetics. If k_{-1} [H_2O] >> k_2, the reaction involves a rapid preequilibrium step followed by slow unimolecular elimination from the carbanion: the mechanism is termed $(E1cB)_R$, and its rate is represented by Eq. 18:

$$\text{rate}(E1cB)_R = \frac{k_1\, k_2[CF_3CF_2CHCl_2][OH^-]}{k_{-1}[H_2O]} \quad (18)$$

If k_2 >> k_{-1}[H_2O], proton abstraction is rate-limiting, and the resulting carbanion decomposes unimolecularly to an alkene more rapidly than it undergoes protonation by water; the mechanism is termed $(E1cB)_I$ and its rate is represented by Eq. 19:

$$\text{rate}(E1cB)_I = k_1\,[CF_3CF_2CHCl_2][OH^-] \quad (19)$$

As shown above (Table S8), the $\Delta S^{\ddagger}$ values obtained for aqueous reactions of $CF_3CF_2CHCl_2$ with OH^- were positive. However, typical values of $\Delta S^{\ddagger}$ for the E2 and $(E1cB)_I$ mechanisms are reported to be much more negative [*12*] because the transition state includes association of reactants. In contrast, positive or near-zero values of $\Delta S^{\ddagger}$ have been reported for the $(E1cB)_R$ mechanism [*12*, *13*, *14*] as $k_{OH^-} = k_1\, k_2 / (k_{-1}[H_2O])$. Accordingly, aqueous reactions of $CF_3CF_2CHCl_2$ with OH^- probably proceed through base-promoted $(E1cB)_R$-type dehydrofluorination such as $CF_3CF_2CHCl_2 + OH^- \rightleftarrows H_2O + [CF_3CF_2CCl_2]^- \rightarrow H_2O + CF_3CF{=}CCl_2 + F^-$.

In contrast, aqueous reactions of CF_3CHCl_2 with OH^- cannot proceed through such dehydrofluorination as that observed for $CF_3CF_2CHCl_2$. The reason is unclear. The large negative $\Delta S^{\ddagger}$ for aqueous reactions of CF_3CHCl_2 with OH^- implies that the reaction may proceed through an E2 or $(E1cB)_I$ mechanism or other mechanism such as nucleophilic substitution by OH^-.

Implications of the results for ODS destruction technology

The hydrolysis of six kinds of commercial HCFCs was examined, and hydrolysis was observed only for $CF_3CF_2CHCl_2$ and CF_3CHCl_2 under the experimental conditions examined. $CF_3CF_2CHCl_2$ and CF_3CHCl_2 have the common group $CHCl_2$ in their molecular structures. Whereas the solubility of $CF_3CF_2CHCl_2$ in water at 353 K was four times smaller than that of CF_3CHCl_2, the hydrolysis rate of $CF_3CF_2CHCl_2$ at 353 K was 10^3 larger than that of CF_3CHCl_2.

From the viewpoint of ODS destruction technology, hydrolysis would not be an effective technique for destruction of CH_3CCl_2F, CH_3CClF_2, CF_3CHClF, or $CClF_2CF_2CHClF$. For CF_3CHCl_2, the k_{OH^-} value at 353 K is 10^3 times smaller than that of $CF_3CF_2CHCl_2$ or $CHClF_2$; hence, hydrolysis would not be an effective technique for destruction of CF_3CHCl_2 unless the reaction is accelerated by catalysis.

In contrast, because the k_{OH^-} value at 353 K of $CF_3CF_2CHCl_2$ is as large as that of $CHClF_2$, hydrolysis could be a potential technique for destruction of $CF_3CF_2CHCl_2$ as well as $CHClF_2$. However, efficient destruction of $CF_3CF_2CHCl_2$ is currently limited by two outstanding issues that must be addressed in order to effectively destroy $CF_3CF_2CHCl_2$ via hydrolysis. First, because the K_H value at 353 K of $CF_3CF_2CHCl_2$ is 7 times smaller than that of $CHClF_2$ (*3*), greater dissolution of $CF_3CF_2CHCl_2$ in water will be required to achieve an HCFC removal rate similar to that of $CHClF_2$. Second, because the degradation product $CF_3CF{=}CCl_2$ is formed and remains present throughout the hydrolysis of $CF_3CF_2CHCl_2$, reaction conditions under which the formation of $CF_3CF{=}CCl_2$ is decreased are required. Alternatively, an additional technique for destroying $CF_3CF{=}CCl_2$ are required.

Conclusion

The K_H values of six kinds of commercial HCFCs were determined at 313–353 K by means of a phase-ratio variation headspace method. The K_H values, in M atm^{-1}, determined at 353 K were 0.0070 ± 0.0006 (CH_3CCl_2F), 0.0038 ± 0.0011 (CH_3CClF_2), 0.0065 ± 0.0007 (CF_3CHCl_2), 0.0026 ± 0.0007 (CF_3CHClF), 0.0016 ± 0.0003 ($CF_3CF_2CHCl_2$), and 0.0022 ± 0.0004 ($CClF_2CF_2CHClF$). Errors represent two standard deviations only for the fitting. Values of enthalpy of dissolution in water ranged from –21 to –30 kJ mol^{-1}. The K_H values determined for CH_3CClF_2, CF_3CHCl_2, and CF_3CHClF were in agreement with the reported values (*6*, *7*), whereas the K_H values determined for CH_3CCl_2F were an order of magnitude larger than the values reported in the literature (*6*). The reported K_H values of CH_3CCl_2F might have been underestimated. To the author's knowledge, the data shown here are the first reported K_H values for $CF_3CF_2CHCl_2$ and $CClF_2CF_2CHClF$.

Hydrolysis was confirmed only for $CF_3CF_2CHCl_2$ and CF_3CHCl_2 under the reaction conditions examined. Aqueous reactions of $CF_3CF_2CHCl_2$ with OH^- probably proceeded through reversible E1cB-type dehydrofluorination such as $CF_3CF_2CHCl_2 + OH^- \rightleftarrows H_2O + [CF_3CF_2CCl_2]^- \rightarrow H_2O + CF_3CF{=}CCl_2 + F^-$. The k_{OH}-(T) values at 313–353 K were determined to be $(0.575 \pm 0.043) \times \exp[-(11300 \pm 620) \times (T^{-1} - 1/353)]$ M^{-1} s^{-1} for $CF_3CF_2CHCl_2$ and $(2.90 \pm 0.15) \times 10^{-4} \times \exp[-(8770 \pm 910) \times (T^{-1} - 1/353)]$ M^{-1} s^{-1} for CF_3CHCl_2. To the author's knowledge, the data shown here are the first reported $k_{OH^-}(T)$ values for $CF_3CF_2CHCl_2$ and CF_3CHCl_2.

The k_{OH^-} value at 353 K of $CF_3CF_2CHCl_2$ was as large as that of $CHClF_2$; therefore, hydrolysis could be a potential technique for destruction of both $CF_3CF_2CHCl_2$ and $CHClF_2$. However, the limited solubility of $CF_3CF_2CHCl_2$ in water, as well as the formation of the degradation product $CF_3CF{=}CCl_2$, must be addressed in order to achieve efficient hydrolysis. The k_{OH^-} value at 353 K of CF_3CHCl_2 was 10^3 times smaller than that of $CF_3CF_2CHCl_2$ or $CHClF_2$ although the activation energy of the former was lowest among these HCFCs; hence, catalysis may be necessary to apply hydrolysis to destruction of

CF_3CHCl_2. Reaction mechanisms for aqueous reactions with OH^- differed between $CF_3CF_2CHCl_2$ and CF_3CHCl_2: a reversible E1cB-type dehydrofluorination occurred only in aqueous reactions of $CF_3CF_2CHCl_2$ with OH^-.

Acknowledgement

This study was supported by research grants from the Steel Foundation for Environmental Protection Technology, Japan.

REFERENCES

(1) IPCC/TEAP In IPCC/TEAP Special Report on Safeguarding the Ozone Layer and the Global Climate System: Issues Related to Hydrofluorocarbons and Perfluorocarbons. Prepared by Working Group I and III of the Intergovernmental Panel on Climate Change, and the Technology and Economic Assessment Panel; Metz, B., Kuijpers, L., Solomon, S., Andersen, S. O., Davidson, O., Pons, J., de Jager, D., Kestin, T., Manning, M., Meyer, L. A., Eds.; Cambridge University Press: Cambridge, United Kingdom and New York, NY, USA, 2005; p 488.

(2) UNEP "Handbook for the Montreal Protocol on Substances that Deplete the Ozone Layer - 8th Edition," 2009, http://www.unep.ch/ozone/Publications/MP_Handbook/MP-Handbook-2009.pdf

(3) Kutsuna, S.; Hori, H.; Naganuma, M.; Shimono, A. International Journal of Chemical Kinetics 2011, 43, 639-647.

(4) Ettre, L.; Welter, C.; Kolb, B. Chromatographia 1993, 35, 73-84.

(5) Chai, X.-S.; Falabella, J. B.; Teja, A. S. Fluid Phase Equilibria 2005, 231, 239-245.

(6) McLinden, M. O. Physical properties. In vol. II, Appendix AFEAS report, WMO Global Ozone Res. Monit. Proj. Rep. 20; WMO: Geneva, 1989; pp 10-38.

(7) Chang, W.-K.; Criddle, C. S. Biodegradation 1995, 6, 1-9.

(8) Banks, R. E.; Barlow M. G.; Nickkho-Amiry M. J. Fluorine Chemistry 1997, 82, 171-174.

(9) Amii, H.; Uneyama, K. Chemical Review 2009, 100, 2119-2183.

(10) Bartsch, R. A.; Závada, J. Chemical Review 1980, 80, 453-494.

(11) Washington, J. W. Ground Water 1996, 34, 709-718.

(12) Spillane, W. J.; McGrath, P.; Brack, C.; Barry, K. Chemical Communication, 1998, 1017-1018.

(13) Nome, F.; Erbs, W.; Correia, V. R. Journal of Organic Chemistry, 1981, 46, 3802-3804.

(14) Vigroux, A.; Bergon, M.; Bergonzi, C.; Tisnès, P. Journal of the American Chemical Society, 1994, 116, 11787-11796.

Table I. Henry's law constants of HCFCs: parameters deduced from fitting the K_H values obtained in this study with Eq. 3. The corresponding values in the literature are also listed.

HCFCs	This study			Literature data		
	K_H (M atm^{-1})		ΔH_{sol} (kJ mol^{-1})	K_H(298) (M atm^{-1})	ΔH_{sol} (kJ mol^{-1})	Ref.
	298 K	353 K				
CH_3CCl_2F	0.030 ± 0.002	0.0070 ± 0.0006	–23 ± 2	0.008	–44	6
CH_3CClF_2	0.015 ± 0.007	0.0038 ± 0.0011	–22 ± 10	0.014	–21	6
				0.016	–25	7
CF_3CHCl_2	0.023 ± 0.003	0.0065 ± 0.0007	–21 ± 3	0.029	–21	6
				0.034	–28	7
CF_3CHClF	0.011 ± 0.003	0.0026 ± 0.0007	–23 ± 8	0.011	–27	6
$CF_3CF_2CHCl_2$	0.010 ± 0.002	0.0016 ± 0.0003	–30 ± 4			
$CClF_2CF_2CHClF$	0.011 ± 0.002	0.0022 ± 0.0003	–25 ± 4			

Table II. Rate constants (k_{OH^-}) for aqueous reactions of $CF_3CF_2CHCl_2$ and CF_3CHCl_2 with OH^-, determined from Eqs. 4′ and 8 at five temperatures, and values extrapolated to 298 K, along with activation energies ΔE_a.

T (K)	k_{OH^-} (10^{-3} M^{-1} s^{-1})			
	$CF_3CF_2CHCl_2$		CF_3CHCl_2	
	From Eq. 4′	From Eq. 8	From Eq. 4′	From Eq. 8
353	651.2 ± 54.4	569.6 ± 48.5	0.332 ± 0.017	0.284 ± 0.015
343	293.4 ± 22.8	228.0 ± 20.7	0.201 ± 0.009	0.152 ± 0.011
333	126.6 ± 7.8	84.9 ± 6.7	0.069 ± 0.012	0.048 ± 0.017
323	51.5 ± 6.8	26.7 ± 7.8	0.022 ± 0.020	0.016 ± 0.018
313	24.9 ± 10.4	9.2 ± 13.3	0.020 ± 0.014	0.006 ± 0.025
298	4.3 ± 0.8	1.6 ± 0.4	0.006 ± 0.002	0.003 ± 0.001
ΔE_a (kJ mol^{-1})	79.6 ± 4.0	93.9 ± 5.1	64.5 ± 5.0	72.9 ± 7.5

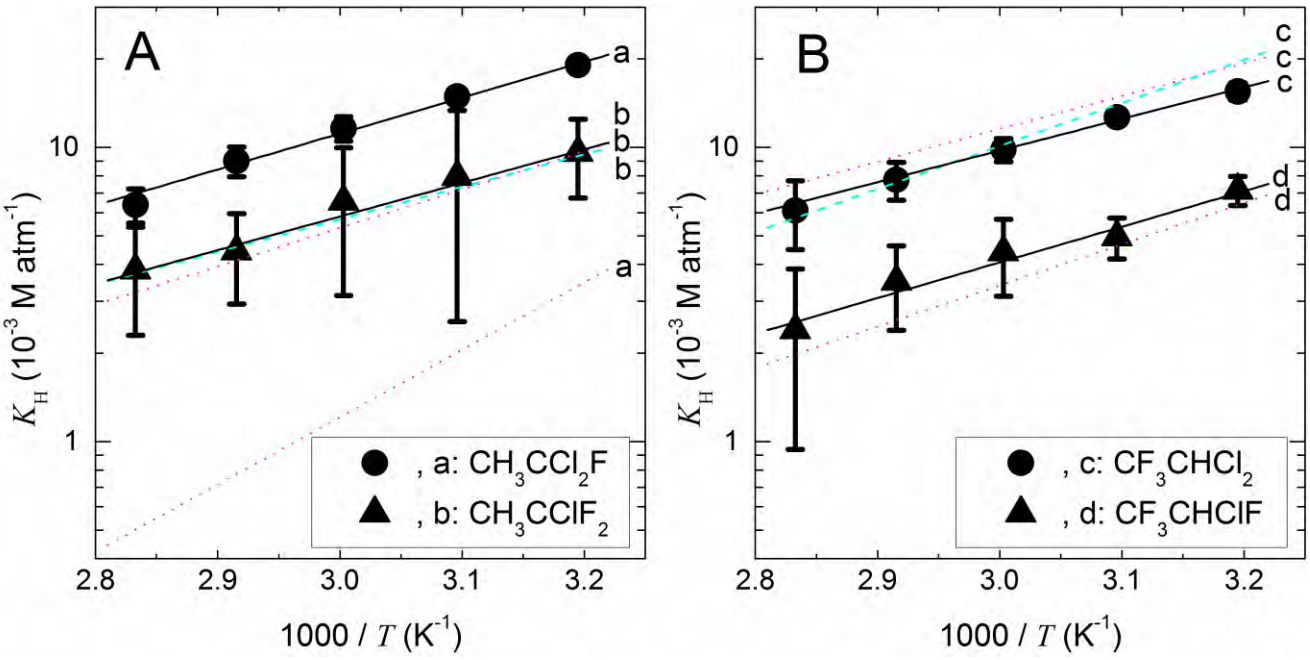

Figure 1. Temperature dependence of Henry's law constants (K_H) determined at 313–353 K: (panel A) CH_3CCl_2F and CH_3CClF_2; (panel B) CF_3CHCl_2 and CF_3CHClF. Bold lines were obtained by nonlinear fitting of the data with respect to Eq. 3. Dashed and dotted lines were obtained on the basis of the data reported in the literature: dashed lines, Ref. 6; dotted lines, Ref. 7.

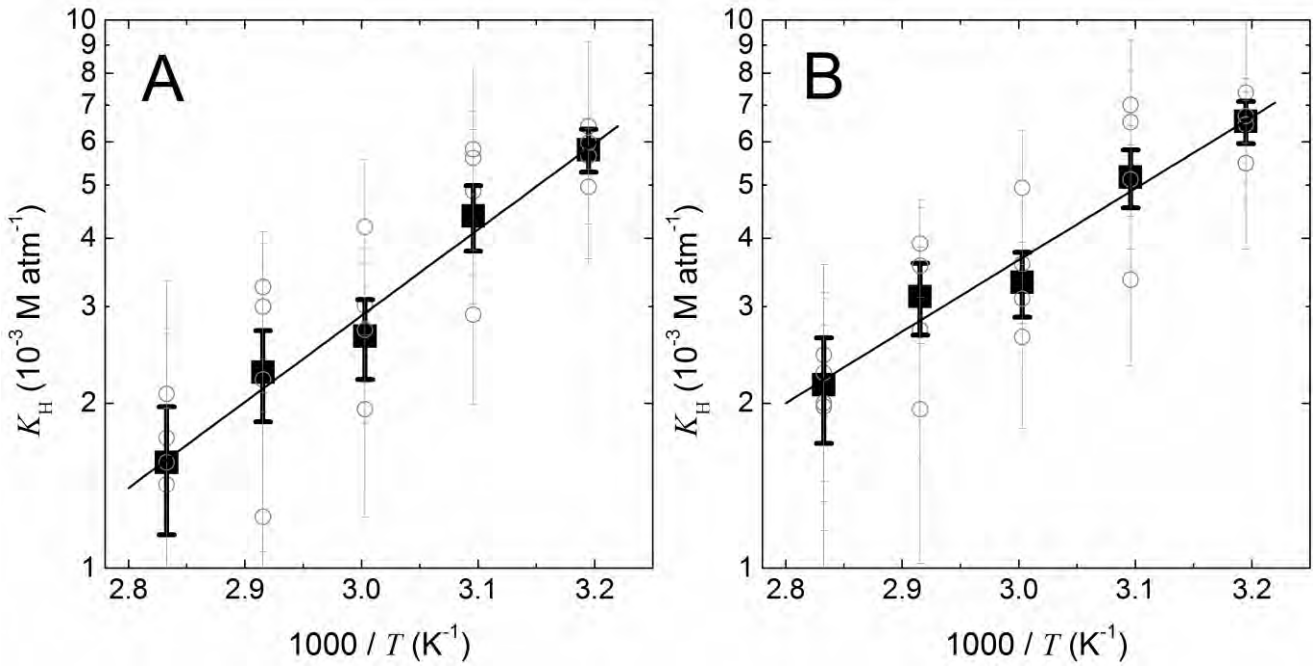

Figure 2. Temperature dependence of Henry's law constants (K_H) determined at 313–353 K: (panel A) $CF_3CF_2CHCl_2$; (panel B) $CClF_2CF_2CHClF$. Bold lines were obtained by nonlinear fitting of the data with respect to Eq. 3. The data at 328, 338 and 353 K are the average obtained in two experimental determinations at each temperature (gray open square symbols and error bars).

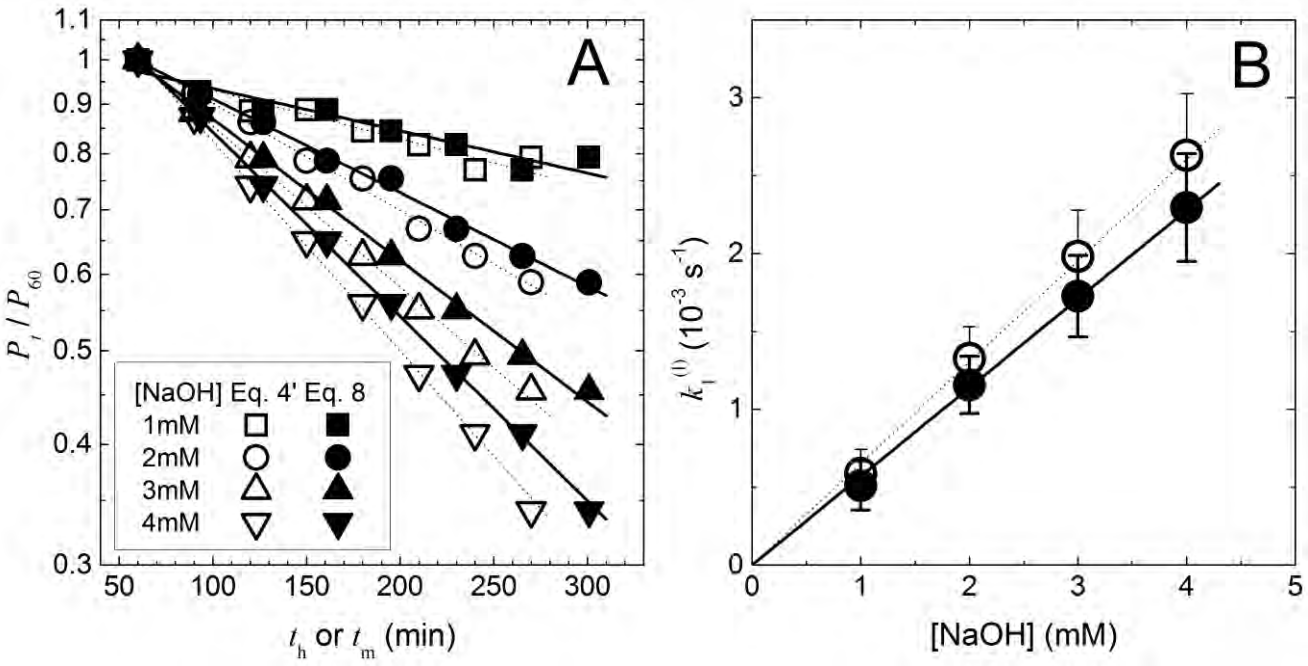

Figure 3. Semi-log plots of relative headspace partial pressure of each HCFC against headspace equilibrium time duration (t_h) at 353 K for V_i = 9.0 cm^3 of 1 M aqueous NaOH.

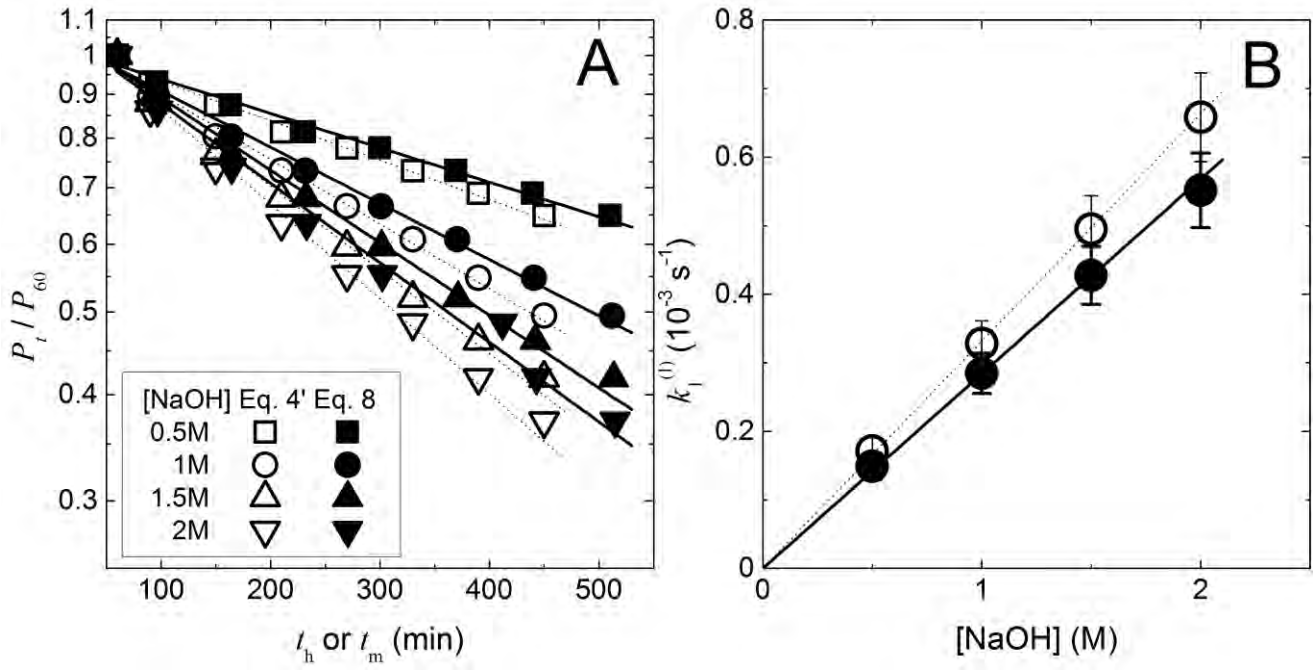

Figure 4. Aqueous reactions of $CF_3CF_2CHCl_2$ with OH^- at 353 K. (panel A) Headspace partial pressure of $CF_3CF_2CHCl_2$ over 9 cm^3 of 1–4 mM aqueous NaOH versus t_h (open symbols) or t_m (closed symbols). (panel B) $k_1^{(l)}$, which were deduced from the data in panels A by Eq. 4′ (open symbols) and Eq. 8 (closed symbols), versus the NaOH concentration.

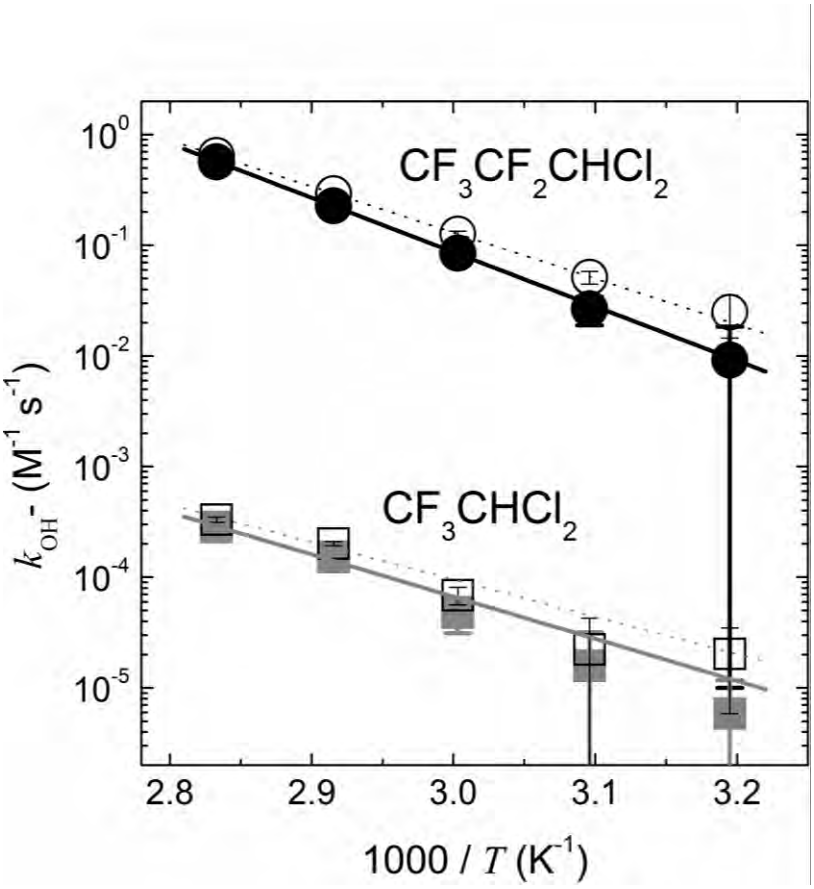

Figure 5. Temperature dependence of the k_{OH^-} values of $CF_3CF_2CHCl_2$ (circles) and CF_3CHCl_2 (squares). Open symbols represent the k_{OH^-} values deduced by use of Eq. 4'. Closed symbols represent the k_{OH^-} values, which considered hydrolysis at room temperature, deduced by used of Eq. 8. Dashed and bold lines were obtained by nonlinear fitting of the data with weighting $(error)^{-2}$ with respect to Eq. 11.

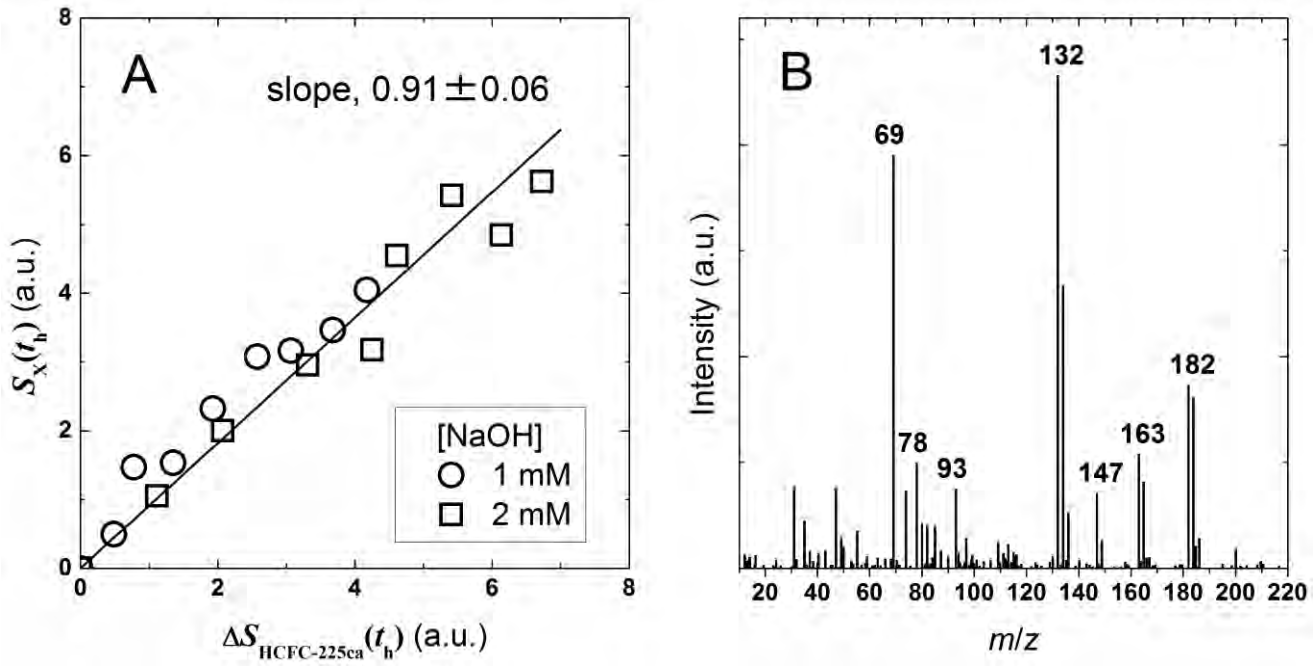

Figure 6. (panel A) FID signal intensities of a degradation product, denoted *product X*, and ddecay of $CF_3CF_2CHCl_2$ at headspace time duration of t_h. Headspace test samples containing 9 cm^3 of 1 or 2 M aqueous NaOH were used for FID-GC measurements. $S_X(t_h)$ and $\Delta S_{HCFC\text{-}225ca}(t_h)$ represent FID signal intensity of a degradation product and decrease in FID signal intensity of $CF_3CF_2CHCl_2$, respectively, at headspace time duration of t_h. (panel B) Mass spectrum of *product X*, which was a degradation product of aqueous reactions of $CF_3CF_2CHCl_2$ with OH^- at 353 K, measured by use of GC-MS.

Supporting Information

1. Time for equilibration

The time to attain equilibration between the headspace and the aqueous solution was obtained by analyzing the headspaces over test samples as a function of headspace time duration until steady state conditions were attained. Figure S1 plots relative peak area of the GC-MS signal versus headspace time duration for each series of test samples.

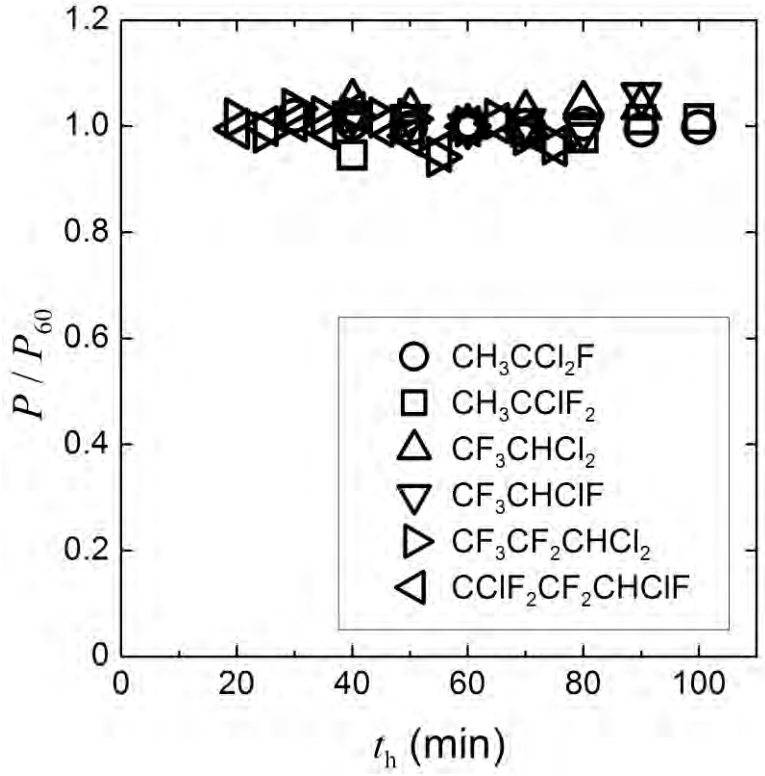

Figure S1. Relative peak area of GC-MS signal vs. headspace time duration for equilibrating 9.0 cm^3 volumes of aqueous solutions of each HCFC at 353 K.

2. Analytical conditions of GC-MS

Table S1 lists the analytical conditions of the selected-ion and the column temperature for each HCFC in GC-MS measurements.

Table S1. Analytical conditions of GC-MS (selected ion and column temperature control)

HCFC	Selected ion (m/z)	Column temperature (K)			Retention time (min)
		Initial (duration)	Rising rate (K min^{-1})	Final	
PoraBOND-Q					
CH_3CCl_2F	CH_3CClF^+ (81)	393 (2 min)	20	453	9.6
CH_3CClF_2	$CH_3CF_2^+$ (65)	313 (3 min)	10	473	14.4
CF_3CHCl_2	$CHCl_2^+$ (83)	393 (2 min)	20	453	9.5
CF_3CHClF	$CHClF^+$ (67)	313 (3 min)	10	473	14.6
$CF_3CF_2CHCl_2$	$CHCl_2^+$ (83)	393 (2 min)	20	493	10.01
$CClF_2CF_2CHClF$	$CHClF^+$ (67)	393 (2 min)	20	493	10.18
Rts-1					
$CF_3CF_2CHCl_2$	CF_3^+ (69)	308 (12 min)	0	308	8.6
$CClF_2CF_2CHClF$	CCl_2F^+ (85)	308 (12 min)	0	308	9.4

3. Linear regression of plots of reciprocal L_i versus phase-ratio with Eq. 3

Fig. S2 shows plots of S_{ij} versus v_j (panel A) and a plot of L_i^{-1} versus V_i / V (panel B) for samples of CH_3CCl_2F at 343 K as an example for determining the Henry's law constant by use of Eqs 2 and 3.

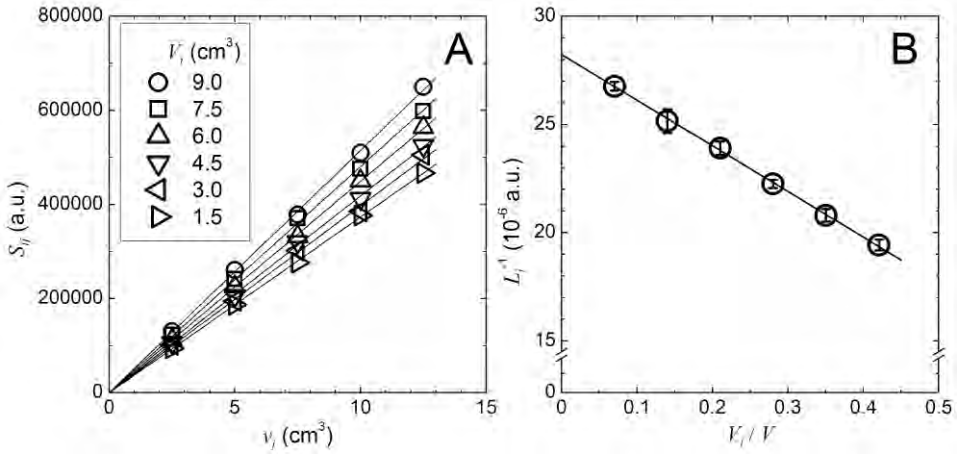

Figure S2. Headspace GC-MS measurements for six series of test samples containing water (V_i cm^3) and CH_3CCl_2F (v_j cm^3) at 343 K. (A) Peak area (S_{ij}) versus v_j for test samples containing each volume (V_i) of water. Slope L_i was obtained by linear fitting of the data with respect to Eq. 2 for samples of the same V_i. (B) Plot of L_i^{-1} against V_i / V with respect to Eq. 3.

4. Henry's law constants of HCFCs obtained at 353– 313 K by use of Eq. 3

Tables S2, S3, S4, S5, S6 and S7 list the values for CH_3CCl_2F, CH_3CClF_2, CF_3CHCl_2, CF_3CHClF, $CF_3CF_2CHCl_2$, $CClF_2CF_2CHClF$, respectively, of reciprocal L_i values, slopes and intercepts and correlation coefficients (r^2) for linear regression of plots of reciprocal L_i versus phase ratio (V_i/V) with weighting (error)$^{-2}$ with respect to Eq. 3, and Henry's law constants (K_H) calculated from the slopes and intercepts. The data were obtained by intervals of 10 K. The average K_H values obtained in four experimental determinations with weighting (error)$^{-2}$ at each temperature were listed for $CF_3CF_2CHCl_2$ (Table S6) and $CClF_2CF_2CHClF$ (Table S7).

Table S2. L_i^{-1}, and slopes, intercepts and correlation coefficients for linear regression of plots of L_i^{-1} versus phase ratio with respect to Eq. 3, and K_H for CH_3CCl_2F at 313– 353 K.

T (K)	353	343	333	323	313
L_i^{-1}(10^{-5} a.u.)					
V_i = 9.0	2.102 ± 0.020	1.943 ± 0.025	1.974 ± 0.021	1.995 ± 0.020	1.993 ± 0.006
V_i = 7.5	2.273 ± 0.038	2.080 ± 0.029	2.078 ± 0.019	2.099 ± 0.006	2.112 ± 0.022
V_i = 6.0	2.427 ± 0.044	2.226 ± 0.019	2.241 ± 0.018	2.232 ± 0.006	2.178 ± 0.019
V_i = 4.5	2.620 ± 0.042	2.391 ± 0.031	2.337 ± 0.041	2.319 ± 0.016	2.259 ± 0.019
V_i = 3.0	2.834 ± 0.012	2.516 ± 0.054	2.495 ± 0.025	2.449 ± 0.014	2.358 ± 0.020
V_i = 1.5	2.982 ± 0.036	2.677 ± 0.019	2.621 ± 0.027	2.543 ± 0.018	2.449 ± 0.021
Slope (10^{-5} a.u.)	–2.601 ± 0.077	–2.109 ± 0.081	–1.879 ± 0.082	–1.616 ± 0.048	–1.296 ± 0.046
Intercept (10^{-5} a.u.)	3.191 ± 0.019	2.823 ± 0.022	2.755 ± 0.024	2.675 ± 0.014	2.540 ± 0.017
r^2	0.99829	0.99944	0.99622	0.99311	0.99785
K_H (M atm^{-1})	0.0064 ± 0.0008	0.0090 ± 0.0010	0.0116 ± 0.0011	0.0149 ± 0.0007	0.0191 ± 0.0007

Table S3. L_i^{-1}, and slopes, intercepts and correlation coefficients for linear regression of plots of L_i^{-1} versus phase ratio with respect to Eq. 3, and K_H for CH_3CClF_2 at 313– 353 K.

T (K)	353	343	333	323	313
L_i^{-1}(10^{-5} a.u.)					
V_i = 9.0	1.044 ± 0.015	0.952 ± 0.011	2.715 ± 0.074	1.001 ± 0.060	2.147 ± 0.022
V_i = 7.5	1.137 ± 0.019	1.045 ± 0.029	2.959 ± 0.098	1.073 ± 0.048	2.323 ± 0.031
V_i = 6.0	1.253 ± 0.016	1.145 ± 0.025	3.187 ± 0.168	1.145 ± 0.046	2.463 ± 0.039
V_i = 4.5	1.349 ± 0.021	1.228 ± 0.026	3.388 ± 0.170	1.224 ± 0.052	2.624 ± 0.042
V_i = 3.0	1.449 ± 0.032	1.324 ± 0.019	3.690 ± 0.140	1.313 ± 0.058	2.831 ± 0.037
V_i = 1.5	1.565 ± 0.026	1.410 ± 0.027	3.907 ± 0.142	1.421 ± 0.071	2.970 ± 0.049
Slope (10^{-5} a.u.)	–1.479 ± 0.071	–1.318 ± 0.061	–3.403 ± 0.374	–1.168 ± 0.207	–2.368 ± 0.225
Intercept (10^{-5} a.u.)	1.664 ± 0.022	1.507 ± 0.020	4.165 ± 0.125	1.480 ± 0.058	3.143 ± 0.074
r^2	0.99909	0.9997	0.99892	0.99316	0.99813
K_H (M atm^{-1})	0.0038 ± 0.0015	0.0045 ± 0.0015	0.0066 ± 0.0034	0.0080 ± 0.0054	0.0096 ± 0.0029

Table S4. L_i^{-1}, and slopes, intercepts and correlation coefficients for linear regression of plots of L_i^{-1} versus phase ratio with respect to Eq. 3, and K_H for CF_3CHCl_2 at 313–353 K.

T (K)	353	343	333	323	313
L_i^{-1}(10^{-5} a.u.)					
V_i = 9.0	1.489 ± 0.020	1.411 ± 0.017	1.792 ± 0.016	0.956 ± 0.008	0.936 ± 0.006
V_i = 7.5	1.593 ± 0.031	1.496 ± 0.023	1.915 ± 0.028	1.028 ± 0.005	0.998 ± 0.013
V_i = 6.0	1.747 ± 0.017	1.622 ± 0.012	2.076 ± 0.005	1.087 ± 0.008	1.051 ± 0.009
V_i = 4.5	1.851 ± 0.035	1.735 ± 0.022	2.190 ± 0.016	1.142 ± 0.009	1.102 ± 0.018
V_i = 3.0	2.010 ± 0.025	1.845 ± 0.015	2.329 ± 0.017	1.211 ± 0.015	1.145 ± 0.009
V_i = 1.5	2.162 ± 0.068	1.997 ± 0.025	2.470 ± 0.022	1.273 ± 0.007	1.201 ± 0.017
Slope (10^{-5} a.u.)	–1.866 ± 0.102	–1.627 ± 0.065	–1.905 ± 0.062	–0.887 ± 0.025	–0.755 ± 0.033
Intercept (10^{-5} a.u.)	2.267 ± 0.031	2.081 ± 0.018	2.605 ± 0.017	1.335 ± 0.007	1.256 ± 0.011
r^2	0.99641	0.99526	0.99663	0.99874	0.99727
K_H (M atm^{-1})	0.0061 ± 0.0016	0.0078 ± 0.0011	0.0098 ± 0.0009	0.0127 ± 0.0007	0.0155 ± 0.0010

Table S5. L_i^{-1}, and slopes, intercepts and correlation coefficients for linear regression of plots of L_i^{-1} versus phase ratio with respect to Eq. 3, and K_H for CF_3CHClF at 313–353 K.

T (K)	353	343	333	323	313
L_i^{-1}(10^{-5} a.u.)					
V_i = 9.0	1.120 ± 0.023	0.954 ± 0.011	0.889 ± 0.014	0.836 ± 0.007	0.753 ± 0.008
V_i = 7.5	1.221 ± 0.021	1.052 ± 0.012	0.977 ± 0.018	0.927 ± 0.008	0.826 ± 0.019
V_i = 6.0	1.331 ± 0.022	1.149 ± 0.008	1.066 ± 0.022	1.007 ± 0.013	0.907 ± 0.016
V_i = 4.5	1.465 ± 0.009	1.252 ± 0.023	1.141 ± 0.018	1.085 ± 0.018	0.948 ± 0.009
V_i = 3.0	1.569 ± 0.020	1.340 ± 0.011	1.226 ± 0.014	1.162 ± 0.013	1.037 ± 0.025
V_i = 1.5	1.715 ± 0.023	1.445 ± 0.021	1.329 ± 0.013	1.241 ± 0.007	1.084 ± 0.004
Slope (10^{-5} a.u.)	–1.693 ± 0.075	–1.385 ± 0.047	–1.239 ± 0.048	–1.149 ± 0.027	–0.939 ± 0.024
Intercept (10^{-5} a.u.)	1.819 ± 0.018	1.537 ± 0.014	1.409 ± 0.013	1.323 ± 0.008	1.150 ± 0.005
r^2	0.99691	0.99978	0.99851	0.99933	0.9984
K_H (M atm^{-1})	0.0024 ± 0.0015	0.0035 ± 0.011	0.0044 ± 0.0013	0.0050 ± 0.0008	0.0072 ± 0.0008

Table S6. L_i^{-1}, and slopes, intercepts and correlation coefficients for linear regression of plots of L_i^{-1} versus phase ratio with respect to Eq. 3, and K_H for $CF_3CF_2CHCl_2$ at 313– 353 K.

T (K)			353		
L_i^{-1}(10^{-5} a.u.)					
V_i = 9.0	3.013 ± 0.029	2.945 ± 0.040	2.181 ± 0.039	2.638 ± 0.022	
V_i = 7.5	3.358 ± 0.056	3.289 ± 0.030	2.366 ± 0.030	2.852 ± 0.040	
V_i = 6.0	3.672 ± 0.007	3.582 ± 0.048	2.593 ± 0.023	3.191 ± 0.019	
V_i = 4.5	4.007 ± 0.053	3.882 ± 0.034	2.812 ± 0.009	3.469 ± 0.022	
V_i = 3.0	4.335 ± 0.0037	4.198 ± 0.014	3.078 ± 0.046	3.780 ± 0.024	
V_i = 1.5	4.698 ± 0.052	4.578 ± 0.008	3.350 ± 0.039	4.083 ± 0.017	
Slope	–4.755 ± 0.133	–4.695 ± 0.076	–3.317 ± 0.125	–4.167 ± 0.145	
Intercept	5.006 ± 0.0377	4.896 ± 0.011	3.530 ± 0.033	4.365 ± 0.036	
r^2	0.9997	0.9967	0.9935	0.9987	average
K_H (M atm^{-1})	0.00173 ± 0.00095	0.00142 ± 0.00054	0.00208 ± 0.00126	0.00156 ± 0.00118	0.00156 ± 0.00041

T (K)			343		
L_i^{-1}(10^{-5} a.u.)					
V_i = 9.0	2.581 ± 0.025	1.519 ± 0.016	1.478 ± 0.033	1.485 ± 0.017	
V_i = 7.5	2.957 ± 0.035	1.615 ± 0.014	1.619 ± 0.020	1.638 ± 0.013	
V_i = 6.0	3.207 ± 0.035	1.792 ± 0.026	1.768 ± 0.018	1.788 ± 0.018	
V_i = 4.5	3.540 ± 0.081	1.964 ± 0.020	1.939 ± 0.004	1.951 ± 0.016	
V_i = 3.0	3.795 ± 0.015	2.103 ± 0.010	2.104 ± 0.012	2.108 ± 0.015	
V_i = 1.5	4.081 ± 0.025	2.280 ± 0.028	2.242 ± 0.024	2.249 ± 0.023	
Slope	–4.235 ± 0.083	–2.191 ± 0.056	–2.265 ± 0.076	–2.209 ± 0.060	
Intercept	4.388 ± 0.020	2.412 ± 0.015	2.415 ± 0.016	2.413 ± 0.017	
r^2	0.9985	0.9946	0.9985	0.9997	average
K_H (M atm^{-1})	0.00124 ± 0.00069	0.00326 ± 0.00085	0.00221 ± 0.00114	0.00300 ± 0.00091	0.00228 ± 0.00043

T (K)			333		
L_i^{-1}(10^{-5} a.u.)					
V_i = 9.0	2.517 ± 0.041	3.025 ± 0.068	2.794 ± 0.054	1.370 ± 0.010	
V_i = 7.5	2.762 ± 0.002	3.308 ± 0.050	3.088 ± 0.013	1.506 ± 0.013	
V_i = 6.0	3.007 ± 0.018	3.767 ± 0.094	3.451 ± 0.087	1.641 ± 0.019	
V_i = 4.5	3.343 ± 0.022	3.969 ± 0.129	3.685 ± 0.023	1.803 ± 0.008	
V_i = 3.0	3.580 ± 0.030	4.220 ± 0.020	3.957 ± 0.025	1.934 ± 0.032	
V_i = 1.5	3.858 ± 0.034	4.557 ± 0.068	4.266 ± 0.043	2.101 ± 0.027	
Slope	–3.914 ± 0.076	–4.272 ± 0.178	–4.180 ± 0.100	–2.071 ± 0.052	
Intercept	4.134 ± 0.026	4.826 ± 0.068	4.555 ± 0.029	2.237 ± 0.016	
r^2	0.9980	0.9952	0.9995	0.9992	average
K_H (M atm^{-1})	0.00195 ± 0.00071	0.00419 ± 0.00137	0.00301 ± 0.00083	0.00272 ± 0.00088	0.00265 ± 0.0044

T (K)			323		
L_i^{-1}(10^{-5} a.u.)					
V_i = 9.0	2.425 ± 0.020	2.475 ± 0.061	1.391 ± 0.020	1.341 ± 0.026	
V_i = 7.5	2.734 ± 0.051	2.664 ± 0.055	1.557 ± 0.023	1.504 ± 0.013	
V_i = 6.0	2.966 ± 0.024	2.978 ± 0.071	1.685 ± 0.030	1.621 ± 0.032	
V_i = 4.5	3.214 ± 0.037	3.162 ± 0.046	1.795 ± 0.023	1.752 ± 0.025	
V_i = 3.0	3.427 ± 0.032	3.351 ± 0.096	1.940 ± 0.028	1.869 ± 0.006	
V_i = 1.5	3.734 ± 0.032	3.607 ± 0.102	2.079 ± 0.028	2.017 ± 0.025	
Slope	–3.673 ± 0.092	–3.274 ± 0.254	–1.927 ± 0.082	–1.796 ± 0.056	
Intercept	3.979 ± 0.028	3.844 ± 0.074	2.212 ± 0.024	2.123 ± 0.012	
r^2	0.9982	0.9937	0.9973	0.9976	average
K_H (M atm^{-1})	0.00290 ± 0.00091	0.00560 ± 0.00257	0.00487 ± 0.00144	0.00581 ± 0.00101	0.0439 ± 0.0060

T (K)			313		
L_i^{-1}(10^{-5} a.u.)					
V_i = 9.0	2.405 ± 0.049	2.847 ± 0.065	3.104 ± 0.054	1.347 ± 0.008	
V_i = 7.5	2.648 ± 0.027	3.071 ± 0.129	3.414 ± 0.022	1.471 ± 0.016	
V_i = 6.0	2.868 ± 0.021	3.302 ± 0.123	3.736 ± 0.053	1.598 ± 0.022	
V_i = 4.5	3.074 ± 0.028	3.614 ± 0.088	4.000 ± 0.060	1.720 ± 0.022	
V_i = 3.0	3.347 ± 0.038	3.886 ± 0.087	4.299 ± 0.103	1.852 ± 0.013	
V_i = 1.5	3.582 ± 0.039	4.100 ± 0.117	4.569 ± 0.052	1.965 ± 0.009	
Slope	–3.314 ± 0.130	–3.656 ± 0.298	–4.166 ± 0.170	–1.771 ± 0.032	
Intercept	3.798 ± 0.035	4.376 ± 0.089	4.874 ± 0.054	2.092 ± 0.010	
r^2	0.9978	0.9979	0.9992	0.9998	average
K_H (M atm^{-1})	0.00496 ± 0.00137	0.00640 ± 0.00273	0.00565 ± 0.00141	0.00597 ± 0.00062	0.00580 ± 0.00052

Table S7. L_i^{-1}, and slopes, intercepts and correlation coefficients for linear regression of plots of L_i^{-1} versus phase ratio with respect to Eq. 3, and K_H for $CClF_2CF_2CHClF$ at 313– 353 K.

T (K)			353		
L_i^{-1}(10^{-5} a.u.)					
V_i = 9.0	3.734 ± 0.023	3.644 ± 0.046	2.325 ± 0.036	2.777 ± 0.047	
V_i = 7.5	4.159 ± 0.071	4.048 ± 0.045	2.512 ± 0.034	2.998 ± 0.086	
V_i = 6.0	4.558 ± 0.006	4.407 ± 0.057	2.749 ± 0.023	3.347 ± 0.043	
V_i = 4.5	4.952 ± 0.053	4.773 ± 0.031	2.974 ± 0.021	3.641 ± 0.043	
V_i = 3.0	5.358 ± 0.047	5.169 ± 0.028	3.253 ± 0.044	3.965 ± 0.052	
V_i = 1.5	5.805 ± 0.094	5.646 ± 0.039	3.539 ± 0.034	4.265 ± 0.035	
Slope	–5.841 ± 0.139	–5.583 ± 0.140	–3.466 ± 0.119	–4.295 ± 0.153	
Intercept	6.195 ± 0.040	5.976 ± 0.033	3.731 ± 0.032	4.559 ± 0.019	
r^2	0.9998	0.9971	0.9926	0.9989	average
K_H (M atm^{-1})	0.00197 ± 0.00080	0.00227 ± 0.00083	0.00245 ± 0.00113	0.00200 ± 0.00118	0.00216 ± 0.00047

T (K)			343		
L_i^{-1}(10^{-5} a.u.)					
V_i = 9.0	3.202 ± 0.053	1.503 ± 0.014	1.460 ± 0.035	1.475 ± 0.018	
V_i = 7.5	3.653 ± 0.041	1.586 ± 0.015	1.595 ± 0.016	1.624 ± 0.015	
V_i = 6.0	3.954 ± 0.051	1.766 ± 0.028	1.741 ± 0.022	1.769 ± 0.020	
V_i = 4.5	4.369 ± 0.100	1.930 ± 0.025	1.902 ± 0.011	1.929 ± 0.016	
V_i = 3.0	4.690 ± 0.028	2.066 ± 0.009	2.063 ± 0.013	2.075 ± 0.015	
V_i = 1.5	5.033 ± 0.034	2.236 ± 0.033	2.198 ± 0.023	2.214 ± 0.027	
Slope	–5.105 ± 0.138	–2.100 ± 0.051	–2.181 ± 0.074	–2.134 ± 0.064	
Intercept	5.402 ± 0.033	2.360 ± 0.013	2.361 ± 0.017	2.373 ± 0.018	
r^2	0.9983	0.9939	0.9990	0.9997	average
K_H (M atm^{-1})	0.00195 ± 0.00093	0.00391 ± 0.00079	0.00272 ± 0.00113	0.00356 ± 0.00099	0.00313 ± 0.00047

T (K)			333		
L_i^{-1}(10^{-5} a.u.)					
V_i = 9.0	3.162 ± 0.056	3.352 ± 0.075	3.031 ± 0.061	1.355 ± 0.009	
V_i = 7.5	3.452 ± 0.012	3.656 ± 0.055	3.337 ± 0.013	1.489 ± 0.013	
V_i = 6.0	3.770 ± 0.022	4.152 ± 0.095	3.744 ± 0.061	1.619 ± 0.020	
V_i = 4.5	4.156 ± 0.041	4.366 ± 0.143	3.967 ± 0.035	1.777 ± 0.007	
V_i = 3.0	4.460 ± 0.040	4.630 ± 0.023	4.250 ± 0.027	1.904 ± 0.035	
V_i = 1.5	4.778 ± 0.038	4.999 ± 0.070	4.583 ± 0.038	2.067 ± 0.029	
Slope	–4.747 ± 0.113	–4.567 ± 0.194	–4.401 ± 0.103	–2.013 ± 0.048	
Intercept	5.117 ± 0.035	5.280 ± 0.068	4.880 ± 0.031	2.199 ± 0.015	
r^2	0.9989	0.9940	0.9994	0.9994	average
K_H (M atm^{-1})	0.00264 ± 0.00084	0.00494 ± 0.00136	0.00359 ± 0.00080	0.00310 ± 0.00083	0.00332 ± 0.0045

T (K)			323		
L_i^{-1}(10^{-5} a.u.)					
V_i = 9.0	2.989 ± 0.023	2.726 ± 0.067	1.370 ± 0.014	1.340 ± 0.030	
V_i = 7.5	3.374 ± 0.077	2.911 ± 0.057	1.539 ± 0.024	1.506 ± 0.014	
V_i = 6.0	3.649 ± 0.031	3.249 ± 0.080	1.660 ± 0.032	1.612 ± 0.035	
V_i = 4.5	3.933 ± 0.036	3.436 ± 0.052	1.760 ± 0.021	1.738 ± 0.031	
V_i = 3.0	4.210 ± 0.043	3.640 ± 0.106	1.900 ± 0.030	1.851 ± 0.006	
V_i = 1.5	4.556 ± 0.063	3.912 ± 0.128	2.035 ± 0.027	1.996 ± 0.031	
Slope	–4.431 ± 0.127	–3.437 ± 0.287	–1.871 ± 0.072	–1.703 ± 0.059	
Intercept	4.864 ± 0.041	4.154 ± 0.086	2.165 ± 0.023	2.091 ± 0.012	
r^2	0.9981	0.9919	0.9963	0.9967	average
K_H (M atm^{-1})	0.00336 ± 0.00102	0.00651 ± 0.00269	0.00512 ± 0.00130	0.00700 ± 0.00108	0.0517 ± 0.0063

T (K)			313		
L_i^{-1}(10^{-5} a.u.)					
V_i = 9.0	2.032 ± 0.039	3.119 ± 0.069	3.383 ± 0.056	1.350 ± 0.010	
V_i = 7.5	2.208 ± 0.031	3.350 ± 0.136	3.702 ± 0.022	1.470 ± 0.017	
V_i = 6.0	2.361 ± 0.020	3.585 ± 0.135	4.046 ± 0.057	1.595 ± 0.024	
V_i = 4.5	2.553 ± 0.051	3.916 ± 0.093	4.317 ± 0.064	1.712 ± 0.023	
V_i = 3.0	2.777 ± 0.030	4.204 ± 0.093	4.625 ± 0.113	1.839 ± 0.014	
V_i = 1.5	2.965 ± 0.047	4.434 ± 0.121	4.915 ± 0.054	1.949 ± 0.010	
Slope	–2.696 ± 0.130	–3.823 ± 0.313	–4.366 ± 0.178	–1.717 ± 0.037	
Intercept	3.138 ± 0.036	4.716 ± 0.094	5.234 ± 0.057	2.073 ± 0.011	
r^2	0.9945	0.9978	0.9991	0.9998	average
K_H (M atm^{-1})	0.00548 ± 0.00166	0.00737 ± 0.00265	0.00645 ± 0.00137	0.00668 ± 0.00072	0.00653 ± 0.00058

5. Change as a function of headspace time duration of headspace partial pressures of CH_3CCl_2F, CH_3CClF_2, CF_3CHClF and $CClF_2CF_2CHClF$ over 1M aqueous NaOH at 353 K

Fig. S3 shows change in relative headspace partial pressure of CH_3CCl_2F, CH_3CClF_2, CF_3CHClF and $CClF_2CF_2CHClF$ with headspace equilibrium time duration (t_h) at 353 K for V_i = 9.0 cm^3 of 1 M aqueous NaOH.

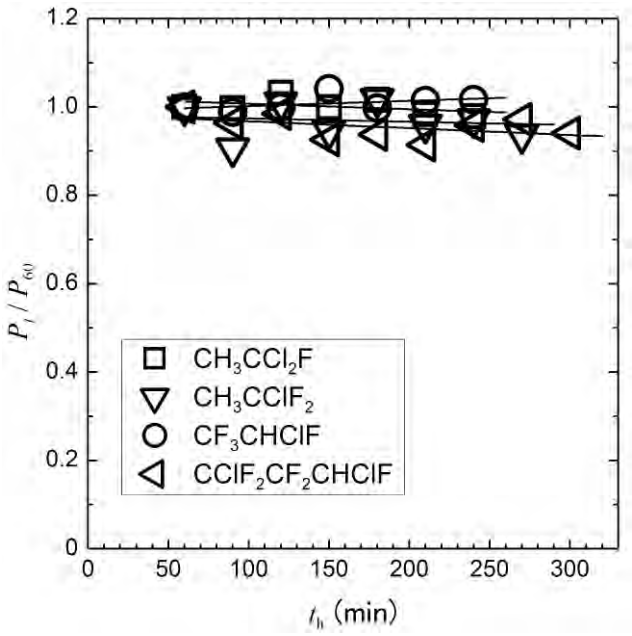

Figure S3. Change of relative headspace partial pressure of HCFC as a function of headspace equilibrium time duration (t_h) at 353 K for V_i = 9.0 cm^3 of 1 M aqueous NaOH.

6. Determination of rate constants for aqueous reactions with OH^- of $CF_3CF_2CHCl_2$ and CF_3CHCl_2

Panels A in Figs. S4 and S5 show plots of P_t/P_{60} of $CF_3CF_2CHCl_2$ and CF_3CHCl_2, respectively, against t_h or t_m over prescribed concentrations of aqueous NaOH at 313–343 K. Panels B in Figs. S4 and S5 show plots of $k_1^{(l)}$, which were deduced from the data in panels A by Eq. 4′ and Eq. 8, of $CF_3CF_2CHCl_2$ and CF_3CHCl_2, respectively, against the NaOH concentration at each temperature.

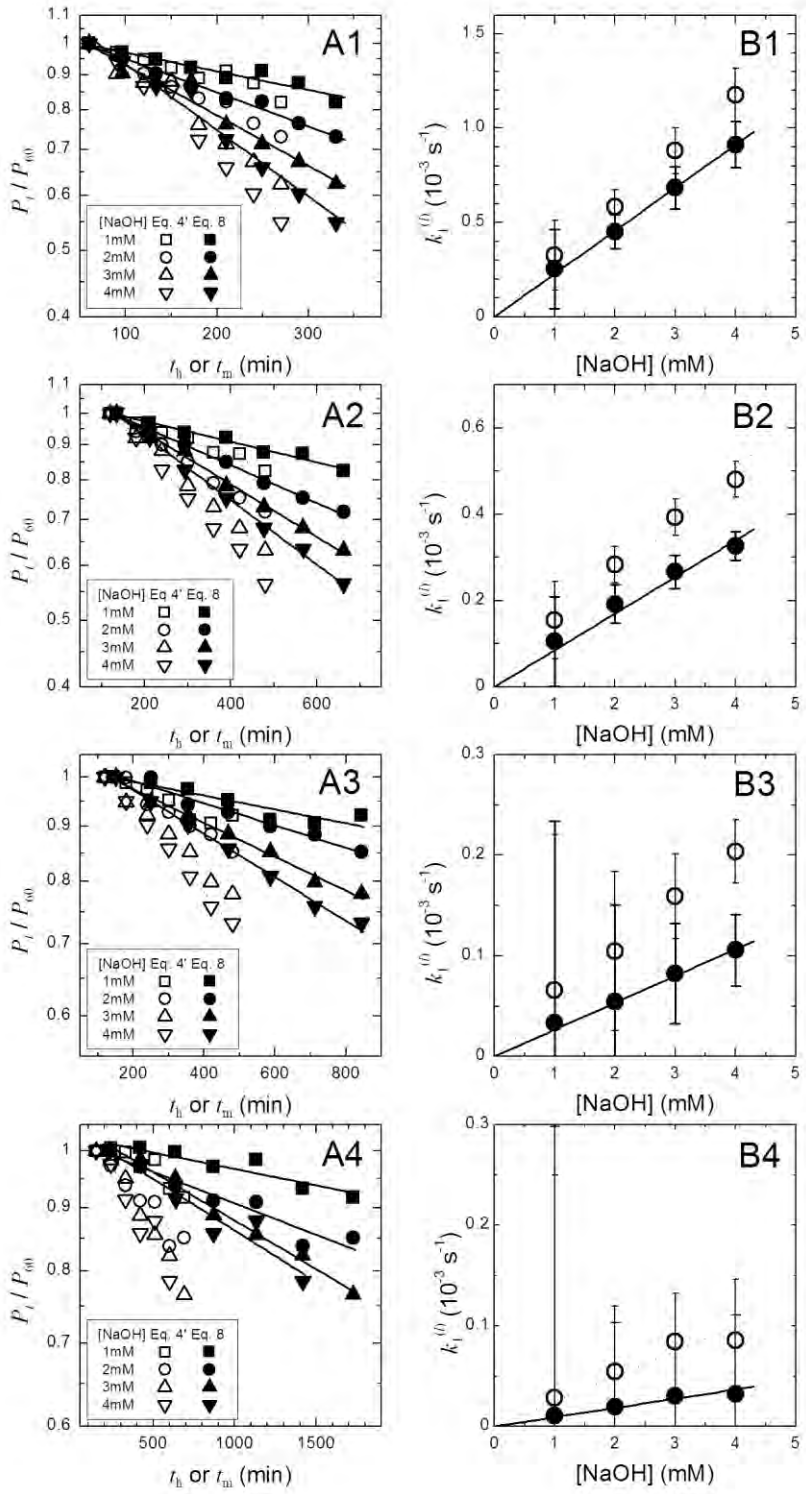

Figure S4. Aqueous reactions of $CF_3CF_2CHCl_2$ with OH^- at 343 K (A1, B1), 333 K (A2, B2), 323 K (A3, B3) and 313 K (A4, B4). Panels A1–A4 plot headspace partial pressure of $CF_3CF_2CHCl_2$ over 9 cm^3 of 1–4 mM aqueous NaOH against t_h (open symbols) or t_m (closed symbols). Panels B1–B4 plot $k_1^{(l)}$, which were deduced from the data in panels A by Eq. 4′ (open symbols) and Eq. 8 (closed symbols), against the NaOH concentration.

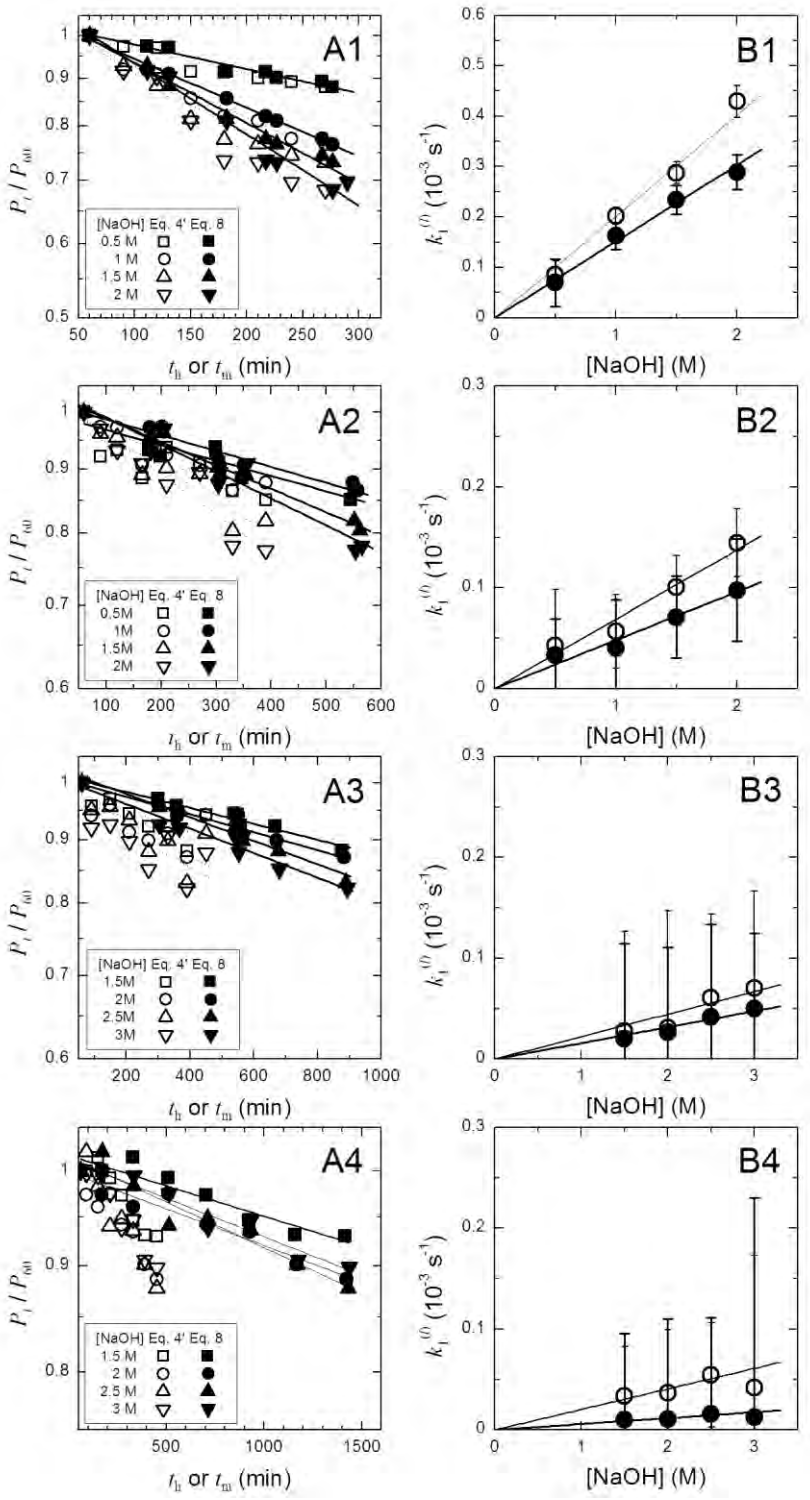

Figure S5. Aqueous reactions of CF_3CHCl_2 with OH^- at 343 K (A1, B1), 333 K (A2, B2), 323 K (A3, B3) and 313 K (A4, B4). Panels A1–A4 plot headspace partial pressure of CF_3CHCl_2 over 9 cm^3 of 0.5–3 M aqueous NaOH against t_h (open symbols) or t_m (closed symbols). Panels B1–B4 plot $k_1^{(l)}$, which were deduced from the data in panels A by Eq. 4′ (open symbols) and Eq. 8 (closed symbols), against the NaOH concentration.

7. Salting-out effect of CF_3CHCl_2 in aqueous NaCl solutions

The salting-out effect was approximately estimated by use of aqueous NaCl solutions instead of aqueous NaOH solutions. Fig. S6 plots change in K_H^{ms} in aqueous NaCl solutions at 313, 333 and 353 K against concentration of NaCl, where K_H^{ms} is an apparent Henry's law constant of CF_3CHCl_2 in a prescribed concentration (m_s) of aqueous NaCl solutions.

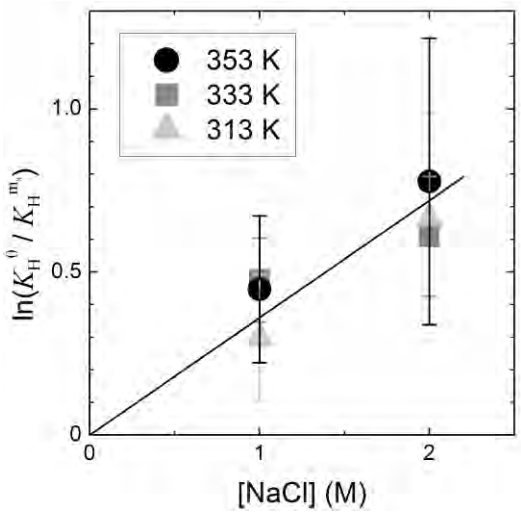

Figure S6. Plots of $\ln(K_H^0 / K_H^{ms})$ versus concentration of aqueous NaCl for evaluating a salting-out effect of CF_3CHCl_2 in aqueous NaCl solutions at 313, 333 and 353 K. The K_H^0 value was deduced from K_H^{353} and ΔH_{sol} listed in Table I with Eq. 3. The K_H^{ms} values were the average obtained in two experiments at each experimental condition (temperature and concentration of NaCl). Five series of headspace samples (total 30 samples) were used to obtain K_H^{ms} under each experimental condition.

8. Comparison of aqueous reactions of OH^- with $CF_3CF_2CHCl_3$ and CF_3CHCl_2

The k_{OH^-} value at 353 K of CF_3CHCl_2 was three orders of magnitude smaller than that of $CF_3CF_2CHCl_2$ although the activation energy for CF_3CHCl_2 was smaller than that for $CF_3CF_2CHCl_2$. Table S8 lists the free energy, the enthalpy and the entropy of activation in aqueous reactions with OH^- of $CF_3CF_2CHCl_2$ and CF_3CHCl_2 with OH^-, calculated from the k_{OH^-} value at each temperature and the activation energy ΔE_a for each reaction.

Table S8. Free energy, enthalpy and entropy of activation in aqueous reactions with OH^- of $CF_3CF_2CHCl_2$ and CF_3CHCl_2 with OH^-, calculated from the k_{OH^-} value at each temperature and the activation energy ΔE_a for each reaction.

T (K)	$CF_3CF_2CHCl_2$			CF_3CHCl_2		
	$\Delta G^‡$ (kJ mol^{-1})	$\Delta H^‡$ (kJ mol^{-1})	$\Delta S^‡$ (J K^{-1} mol^{-1})	$\Delta G^‡$ (kJ mol^{-1})	$\Delta H^‡$ (kJ mol^{-1})	$\Delta S^‡$ (J K^{-1} mol^{-1})
353	88.6	91.0	6.8	110.8	70.0	–115.7
343	88.6	91.0	7.2	109.6	70.0	–115.4
333	88.6	91.1	7.5	108.5	70.1	–115.1
323	89.0	91.2	6.8	107.3	70.2	–114.9
313	88.9	91.3	7.5	106.2	70.3	–114.8